JCTC Journal of Chemical Theory and Computation

Exploring the Limit of Accuracy of the Global Hybrid Meta Density Functional for Main-Group Thermochemistry, Kinetics, and Noncovalent Interactions

Yan Zhao and Donald G. Truhlar*

Department of Chemistry and Supercomputing Institute, University of Minnesota, 207 Pleasant Street S.E., Minneapolis, Minnesota 55455-0431

Received June 25, 2008

Abstract: The hybrid meta density functionals M05-2X and M06-2X have been shown to provide broad accuracy for main group chemistry. In the present article we make the functional form more flexible and improve the self-interaction term in the correlation functional to improve its self-consistent-field convergence. We also explore the constraint of enforcing the exact forms of the exchange and correlation functionals through second order (SO) in the reduced density gradient. This yields two new functionals called M08-HX and M08-SO, with different exact constraints. The new functionals are optimized against 267 diverse main-group energetic data consisting of atomization energies, ionization potentials, electron affinities, proton affinities, dissociation energies, isomerization energies, barrier heights, noncovalent complexation energies, and atomic energies. Then the M08-HX, M08-SO, M05-2X, and M06-2X functionals and the popular B3LYP functional are tested against 250 data that were not part of the original training data for any of the functionals, in particular 164 main-group energetic data in 7 databases, 39 bond lengths, 38 vibrational frequencies, and 9 multiplicity-changing electronic transition energies. These tests include a variety of new challenges for complex systems, including large-molecule atomization energies, organic isomerization energies, interaction energies in uracil trimers, and bond distances in crowded molecules (in particular, cyclophanes). The M08-HX functional performs slightly better than M08-SO and M06-2X on average, significantly better than M05-2X, and much better than B3LYP for a combination of main-group thermochemistry, kinetics, noncovalent interactions, and electronic spectroscopy. More important than the slight improvement in accuracy afforded by M08-HX is the conformation that the optimization procedure works well for data outside the training set. Problems for which the accuracy is especially improved by the new M08-HX functional include large-molecule atomization energies, noncovalent interaction energies, conformational energies in aromatic peptides, barrier heights, multiplicity-changing excitation energies, and bond lengths in crowded molecules.

1. Introduction

The development of new and better exchange-correlation functionals for density functional theory (DFT) is "promising and charming".[1] We classify functionals as local and nonlocal. In the classification used here, at a given point in space, local density functionals depend on at most the spin densities and their derivatives and spin kinetic energy density at that point in space; nonlocal functionals involve an integral over all space. The only widely studied (to date) method to include nonlocality is to incorporate Hartree−Fock (HF) exchange; functionals involving HF exchange are called hybrid. In order of increasing complexity and accuracy, the three types of functionals that we classify as local are the local spin density approximation (LSDA),[2] generalized gradient approximation (GGA),[3−8] and meta-GGAs.[9−13] Nonlocal functionals include hybrid GGAs and hybrid meta

* Corresponding author e-mail: truhlar@umn.edu.

10.1021/ct800246v CCC: $40.75
Published on Web 10/15/2008

functionals. Hybrid GGAs (which include nonlocal HF exchange) have better performance for general-purpose applications in chemistry than the local functionals. One hybrid GGA, namely B3LYP,[4,5,14,15] has become extraordinarily popular.[16] Some later hybrid GGAs, though, such as mPW1PW,[17] PBEh,[18] and B97−3[19] (and, for barriers and noncovalent interactions, MPW1K[20]), have better performance than B3LYP. Hybrid meta density functionals[9,21−28] in which the energy depends on the occupied orbitals not only through the HF exchange terms (as in hybrid GGAs) but also through the noninteracting spin kinetic energy densities[29−32] (as in meta-GGAs) have been shown to be capable of even better performance than hybrid GGAs.[13,23−28] To distinguish them from some new developments mentioned below, conventional hybrid GGAs and hybrid meta functionals may be called global hybrid functionals and global hybrid meta functionals, respectively.

Recently, evidence disparaging the performance of popular density functionals for many areas in chemistry has been presented by many research groups.[33−49] In order to improve the performance of conventional density functionals, besides the design and semiempirical fitting conventional exchange-correlation functionals, four newer approaches have been proposed, namely.

1) DFT-D: DFT-D augments the DFT energy by a damped dispersion term (in the functional or added to the energy as in combined quantum mechanical and molecular mechanical methods) that yields the correct asymptotic form $-C_6R^{-6}$ (plus possibly higher order terms, if the multipole expansion is not truncated at the first term) of the interatomic or intermolecular interaction potential.[50−65] Some recent successful DFT-D functionals are TPSS-D,[53] B97-D,[52,64] and DF07.[65]

2) Range-separated hybrid (RSH) functionals: The RSH approach was first proposed by Savin;[66] in this approach the Coulomb operator is partitioned into long-range and short-range parts, and different treatments are employed for the long-range and short-range operators. Some recent functionals of this type are HSE03,[67] CAM-B3LYP,[68] RSHXPBE,[69] LC-ωPBE,[70] LCgau-BOP,[71] PBE/CCSD,[72] and ωB97X.[73]

3) Local hybrid functionals: the amount of exact HF and DFT exchange in the local hybrid functional, unlike the global hybrid functional, varies according to the local properties of each system.[74] Some developments in refining the local mixing functions have been reported recently.[75−80]

4) Doubly hybrids: A doubly hybrid functional is a hybrid of a global hybrid functional with correlation contributions from unoccupied orbitals. We developed several doubly hybrid models by empirically mixing correlated wave function methods and density functional methods.[81,82] In our published models, we used the HF orbitals for the unoccupied orbitals, although in unpublished work carried out at the time we found that we got similar results for the systems studied by using Kohn−Sham orbitals. In the recent B2PLYP[83] and mPW2PLYP[84] doubly hybrid functionals, Grimme et al. employed the Kohn−Sham unoccupied orbitals to calculate the second-order Møller−Plesset-type perturbation theory correction. (The first-order contribution, which is nonzero when one uses Kohn−Sham orbitals, was omitted.) More recently, Tarnopolsky et al.[85] reoptimized the parameters in B2PLYP and mPW2PLYP for thermochemical kinetics, resulting in the B2K-PLYP and mPW2K-PLYP functionals. Benighaus et al.[86] also optimized a doubly hybrid functional, called B2-P3LYP, and they noted that one major drawback of B2-PLYP or B2-P3LYP is their fifth-order scaling with respect to system size. They proposed a fourth-order scaling doubly hybrid functional, namely B2-OS3LYP, by just retaining the opposite-spin component of the Møller−Plesset-type of correlation energy. Note that these approaches go beyond the hybrid and meta approaches in that they introduce a dependence not only on occupied orbitals but also on the unoccupied-orbital space; as such they are sometimes called fifth-rung[87,88] DFT.

Note that some functionals are developed by combining two of the four approaches, such as the RSE-MP2 functional,[89] which is developed by combining approaches 2) and 4). The B2-PLYP-D and mPW2-PLYP-D functionals were developed by combining approaches 1) and 4).[90]

Among these four kinds of treatments, the range-separated hybrids have a computer cost for molecules that is approximately the same as that of global hybrids, and the HSE functional of Heyd et al.[67] has much improved computational cost for solids. However, the goal of the present study is different from the above-mentioned lines of research. The question we want to address in the present study is the following: *without these nonconventional treatments, how accurate can a global hybrid meta functional be for main-group chemistry*. In particular, what is the limit of accuracy of the global hybrid meta functional form for a combination of three important areas of chemistry:

TC main-group thermochemistry

BH barrier heights

NC noncovalent interactions

We may compare this effort to Becke's work in 1997 and 1998 in which[91,92] he varied parameters to determine the limit of accuracy attainable for TC-type predictions by the hybrid GGA functional form. The final resulting functional, B98, remains to this day a good representative of the best that one can do for main-group thermochemistry with a hybrid GGA.

Recently we have shown that our global hybrid meta M05-2X[27] functional performs well for many problematic systems,[93−100] and this good performance has been confirmed by recent studies from other groups for organic energies,[101] for conjugated addition reaction energetics,[102] for peptides containing an aromatic ring,[103] for the conformational energetics of isocohichine,[104] for excited states of stacked nucleobases,[105] for near-edge X-ray and optical absorption spectra of liquid water,[106] and for the contribution of dipole−dipole interactions to the stability of the collagen triple helix.[107] It is encouraging that these assessments are diverse and outside the training set of M05-2X, showing the transferability of the optimized parameters in the M05-2X functional. Subsequent work showed even an better than average performance by the M06-2X functional,[13,28] which can be considered to be an improved version of M05-2X. M06-2X has been successfully employed to explain the unusual temperature dependence of an atmospherically

Table 1. Basis Set and Geometries

databases	ref	basis sets	geometries
		Training Sets	
MGAE109	27	MG3S	QCISD/MG3
IP13	26,27,113,114	MG3S	QCISD/MG3
EA13	26,27,113,114	MG3S	QCISD/MG3
PA8	93	6−311+G(2df,2p)	MP2(full)/6−31G(2df,p)
ABDE4	11,27,37	6−311+G(3df,2p)	B3LYP/6−31G(d)
πIE3	11,27	6−311+G(2df,2p)	MP2/6−31+G(d,p)
PA-CP5	93	6−311+G(2df,2p)	MP2/6−31+G(d,p)
PA-SB5	93	6−311+G(2df,2p)	MP2/6−31+G(d,p)
DBBH76	27,82,115	MG3S	QCISD/MG3
NCCE31	113,116	MG3S	MC-QCISD/3
AE17	28,117	MQZVP, MG3S, aug-cc-pVQZ[a]	N. A.
		Test Sets	
G3-3AE75	22,33, this work	MG3SXP, 6−311++G(3df,3pd)	B3LYP/6−31G(2df,p)
LMAE14	118, this work	6−311+G(3df,2p)	M06-L/6−311+G(2df,2p)
IE34	119,45	MG3S	B3LYP/TZV(d,p)
S22	120	6−311+G(3df,2p)	WFT
APCE5	121	6−311+G(3df,2p)	RI-MP2/cc-pVTZ
UUU7	122	6−311+G(3df,2p)	RI-MP2/cc-pVTZ
BBH7/08	compiled in this work	6−311+G(3df,2p)	Opt[b]
MGBL24	11,28, this work	MG3S	Opt[b]
CID15	123,124	MG3S	Opt[b]
F38/06	28	MG3S	Opt[b]
MGMCEE9	compiled in this work	aug-cc-pVQZ	experiment + opt[c]

[a] MQZVP is used for training, and MG3S and aug-cc-pVQZ are used for testing. [b] Opt denotes that the geometry is reoptimized for each density functional tested. [c] The molecules for vertical transitions are calculated at fixed geometries as specified in Section 2.2.12, whereas the molecules for adiabatic transitions are reoptimized for each density functional tested with the 6−311+G(2df,2p) basis set.

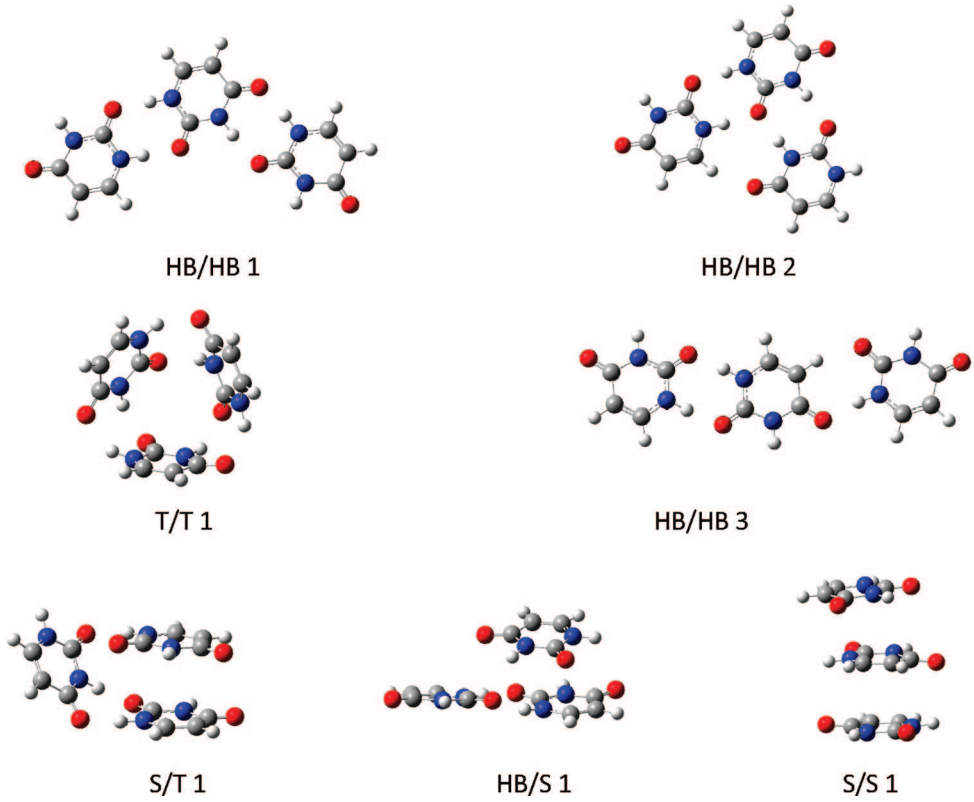

Figure 1. Structures of uracil trimers in the UUU7 database.

important reaction,[108] to study steric isotope effects,[109] to investigate the structures and potential energy surface of coronene dimers,[110] and to calculate host−guest interactions in supramolecular complexes in a hydrocarbon nanoring[111] and concave-convex $\pi...\pi$ interaction in buckyball tweezers.[112] Note that these applications are beyond the reach of the popular functionals. Encouraged by these successes, we investigate in the present study the extent to which further improvements can be achieved using a more flexible functional form (although still of the hybrid meta type), and we call the new functional M08-HX, where "X" is our usual abbreviation for Hartree−Fock exchange, and M08-HX

denotes "Minnesota 2008 high-X". Using the same functional forms as M08-HX, we optimize another functional in which we enforced the gradient expansion to the second order, and we call this functional M08-SO, where SO denotes "second order".

The paper is organized as follows. Section 2 presents our databases. Section 3 gives computational details. Section 4 discusses the theory and parametrization of the new functionals. Section 5 presents results and discussion not only for the TC, BH, and NC areas mentioned above but also for bond lengths, vibrational frequencies, and multiplicity-changing excitation energies. Section 6 concludes the paper.

2. Databases

All databases used in this article are listed in Table 1. Table 1 also presents the references for the databases[11,22,26−28,33,37,45,82,93,113−124] and the basis sets and geometries employed here for each database. The entries in Table 1 are explained in this section. One important difference between the energetic data in the present article and the energetic data used in many other studies is that we exclusively use clamped-nuclei energies (such as equilibrium dissociation energies, D_e, adiabatic clamped-nuclei IPs, or classical barrier heights) rather than 0 K data (such as ground-state dissociation energies, D_0, which include zero point vibrational energy) or 298 K data (such as finite-temperature enthalpies of activation or heats of formation that also include thermal vibrational−rotational energies). Using 0 or 298 K data provides a combined test of the ability to predict electronic, vibrational, and rotational energies (rotational energies depend on geometries). In contrast, by making databases of our best estimates of clamped-nuclei energies (which consist of the electronic energy including nuclear repulsion), we obtain pure tests of Born−Oppenheimer electronic energies. We test vibrational frequencies and bond lengths with separate databases.

2.1. Training Sets. We used the same training sets for M08-HX and M08-SO as for M06-2X,[28] including the MGAE109 database of 109 main-group atomization energies (equilibrium dissociation energies for complete dissociation to ground-state atoms),[27] the IP13 database of 13 ionization potentials, the EA13 database of 13 electron affinities, the PA8 database of 8 proton affinities, the ABDE4 database of four alkyl bond dissociation energies, the DBBH76 database of 76 diverse barrier heights, the πIE3 database of three isomeric energy differences between allene and propyne as well as higher homologues, the PA-CP5/06 database of the proton affinities of five conjugated polyenes, the PA-SB5/06 database of the proton affinities of the five conjugated Schiff bases, the NCCE31 database of 31 noncovalent interaction energies (6 hydrogen bonds, 7 charge transfer complexes, 6 dipole interactions, 7 weak interactions, and 5 π...π interactions), and the AE17 database of 17 nonrelativistic atomic energies[117] for the atoms from H to Cl.

2.2. Test Sets. The training sets for M08-HX and M08-SO consist of mainly small molecules and complexes. We test the functionals outside the training sets and compare the results in all cases with the popular functional B3LYP and the earlier M05-2X functional and in some cases with

Table 2. Optimized Parameters for M08-H and M08-SO

	M08-HX				M08-SO			
i	a_i	b_i	c_i	d_i	a_i	b_i	c_i	d_i
0	2.7925837E+00	−1.7925858E+00	1[a]	1.3812334E+00	−8.0741559E-01	1.8074156E+00	1[a]	1[a]
1	−1.9834852E+01	1.9428586E+01	−4.0661387E-01	−2.4683806E+00	−1.3459249E+01	1.2621657E+01	0[a]	−4.4117403E+00
2	−2.6254749E+01	2.5666211E+01	−3.3232530E+00	−1.1901501E+01	8.6903055E+01	−8.7603211E+01	−3.9980886E+00	−6.4128622E+00
3	1.9127062E+01	−1.1553206E+01	1.5540980E+00	−5.4112667E+01	1.4748300E+02	−1.4416820E+02	1.2982340E+01	4.7583635E+01
4	7.2675747E+01	−7.4387668E+01	4.4248033E+01	1.0055846E+01	−1.2437471E+02	1.0810751E+02	1.0117507E+02	1.8630053E+02
5	1.2315639E+02	−1.7176051E+02	−8.4351930E+01	1.4800687E+02	−2.2817757E+02	2.0208604E+02	−8.9541984E+01	−1.2800784E+02
6	1.4940250E+02	−1.4357663E+02	−1.1955581E+02	1.1561420E+02	3.7681592E+01	3.7152154E+01	−3.5640242E+02	−5.5385258E+02
7	4.8802514E+01	7.5540493E+01	3.9147081E+02	2.5591815E+02	4.0531053E+01	4.6579309E+01	2.0698803E+02	1.3873727E+02
8	1.0114021E+01	−1.9623400E+01	1.8363851E+02	2.1320772E+02	−1.5650903E+01	−9.3366569E+01	4.6037780E+02	4.1646537E+02
9	−1.3616112E+01	−1.2504017E+02	−6.3268223E+02	−4.8412067E+02	2.5703906E+01	−1.3556484E+02	−2.4510559E+02	−2.6626577E+02
10	−2.9429067E+01	3.4724447E+01	−1.1297403E+02	−4.3430813E+02	3.6249816E+00	4.8345920E+01	−1.9638425E+02	5.6676300E+01
11	2.6963722E+01	2.9292867E+01	3.3629312E+02	5.6627964E+01	2.0273888E+01	2.5334189E+01	1.1881459E+02	3.1673746E+02
X	52.23	56.79						

[a] Determined by constraints, as explained in Section 4.4.

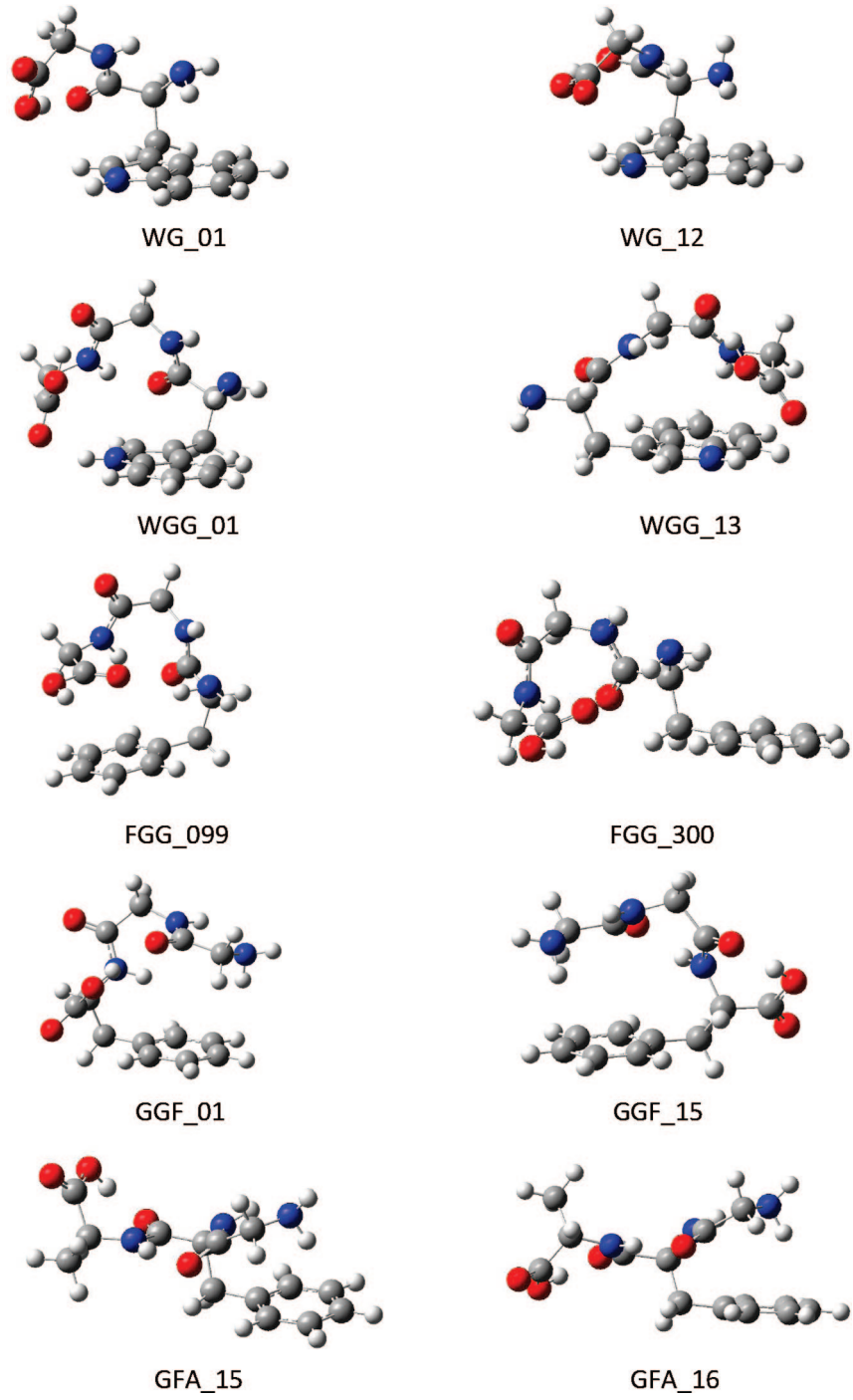

Figure 2. Structures of small peptides in the APCE5 database.

additional selected functionals as well. As indicated in each case, some of the comparison results are taken from the literature, and many others are newly computed especially for this article. The additional databases used for testing are explained next.

2.2.1. G3-3AE75. G3-3AE75 is a database of 75 atomization energies for the molecules in the G3-3 set of Curtiss et al.[33] We used experimental standard enthalpies of formation (at 298 K)[33] and scaled B3LYP/6−31G(2df,p) harmonic zero-point vibration energies (with a scaling factor of 0.9854)[22] and thermal contributions to obtain reference clamped-nuclei experimental atomization energies. This database is given in the Supporting Information.

2.2.2. LMAE14. LMAE14 is a database of 14 large-molecule atomization energies for molecules that have 56 or more valence electrons. Most of the molecules in this set are not feasible for G3 methods.[118] We used experimental standard enthalpies of formation (at 298 K)[118] and scaled M06-L/6−311+G(2df,2p) zero-point vibration energies (with a scaling factor of 0.98) and thermal contributions to obtain reference experimental atomization energies.

2.2.3. IE34. IE34 is a benchmark database of 34 organic isomerization energies compiled by Jorgensen et al.[119,125] Grimme et al.[45] found that four experimental data in this database are not reliable as compared to high-level CCSD(T)

calculations. We use the reference data of Grimme et al.[45] for this database.

2.2.4. S22 Database. The S22 database is a data set of 22 weakly bonded molecular complexes of biological importance. This database was developed by Jurecka et al.,[120] who divided the S22 set into three subsets, namely, 7 hydrogen bonded complexes, 8 dispersion-dominated complexes, and 7 mixed complexes. The reference interaction energies for the S22 data set were calculated[120] by the following scheme

$$\Delta E^{CCSD(T)}CBS = \Delta E^{MP2}CBS + (\Delta E^{CCSD(T)} - \Delta E^{MP2})_{small\ basis} \quad (1)$$

where a complete basis set (CBS) limit CCSD(T) interaction energy is approximated by a CBS MP2 interaction energy plus a difference between CCSD(T) and MP2 interaction energies ($\Delta E^{CCSD(T)} - \Delta E^{MP2}$) evaluated with a relatively small basis set that was specifically designed[126,127] for this purpose. The best estimates of the interaction energies in the S22 database were taken from the paper by Jurecka et al.[120]

2.2.5. UUU7. UUU7 is a benchmark database of 7 noncovalent interaction energies in uracil trimers. The structures for the 7 trimers in UUU7 are shown in Figure 1. The reference data are based on the estimated CCSD(T)/CBS (eq 1) results of Kabelác et al.[122] We used the same name convention as in ref 122 to label these trimers.

2.2.6. APCE5. APCE5 is a benchmark database of 5 aromatic peptide conformational energies in 5 small peptides containing an aromatic side chain, taken from a recent benchmark database compiled by Valdes et al.[121] In particular, APCE5 includes the energy gaps between the highest-energy conformer and the lowest-energy conformer at the estimated CCSD(T)/CBS level for the WG, WGG, FGG, GGF, and GFA peptides containing phenylalanine (F), glycine (G), trypophan (W), and alanine (A). The structures of the 5 pair of peptides are shown in Figure 2, and we use the same name convention in ref 121. The reference conformational energy gaps for the five small peptides are calculated from the estimated CCSD(T)/CBS (eq 1) results of Valdes.[121]

2.2.7. BBH7/08. BBH7/08 is a new (2008) database of 7 diverse benchmark barrier heights in 5 reactions, in particular

$$CH_3 + CH_4 \rightarrow CH_4 + CH_3 \quad (R1)$$

$$HCC + HCCH \rightarrow HCCH + CCH \quad (R2)$$

$$OH^- + CH_3OH \rightarrow CH_3OH + OH^- \quad (R3)$$

$$HCC + H_2 \rightarrow HCCH + H \quad (R4)$$

$$O + CH_4 \rightarrow OH + CH_3 \quad (R5)$$

The reference data for reactions R1, R2, and R4 are based on W1[128] calculations, and they were taken from our previous study.[129] The reference classical barrier height for R3 was taken from a focal point calculation of Gonzales et al.[130] The reference forward and reverse classical barrier heights for R5 are based on the CCSD(T)/CBS calculations by Troya.[131]

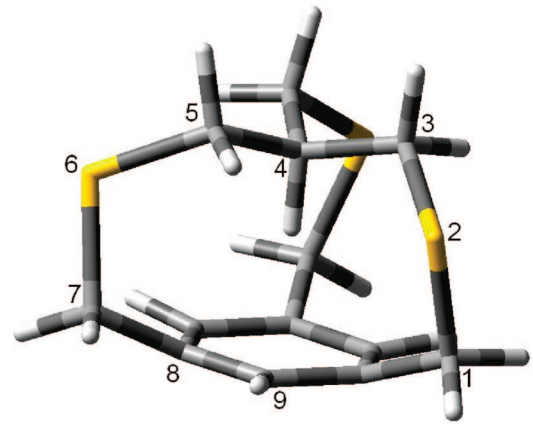

Figure 3. Structure of 2,6,15-trithia-*in*-[$3^{4,10}$][7]metacyclophane.

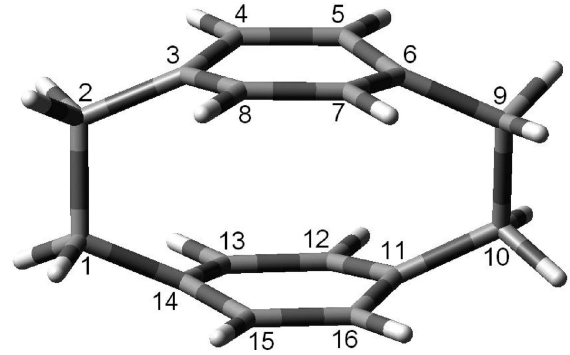

Figure 4. Structure of [2.2]paracyclophane.

2.2.8. MGBL24. MGBL24 is a database of 24 bond lengths in 20 molecules. This database is based on our previous MGBL19 database.[11] We augmented the MGBL19 database by including three main-group metal dimers (Li_2, Na_2, Al_2), an open-shell molecule (BN), and a high-coordination molecule (SF_6). The reference data were taken from Computational Chemistry Comparison and Benchmark Database[132] and from Handy and Tozer.[133]

2.2.9. CID15. CID15 is a database for 15 internuclear distances in two cyclophanes, namely 2,6,15-*in*-trithia[$3^{4,10}$]-[7]metacyclophane and [2,2]paracyclophane. The structures of these molecules are shown in Figures 3 and 4. The reference data were taken from Pascal et al.[123] and Grimme.[124]

2.2.10. F38/06. F38 is a database of 38 harmonic frequencies compiled in a previous study,[28] which consists of the F36/06 database[11] plus the harmonic frequencies[134] of the OH and Cl_2 molecules.

2.2.11. MGMCEE9. MGMCEE11 is a database of 9 main-group electronic excitation energies for transitions to the lowest-energy excited states with a multiplicity different from the ground state, including two atoms (Be and Mg)[28] and seven molecules. Among the seven molecules, we have vertical excitations for five molecules (BeH, CO, H_2CO, H_2O, and N_2) at fixed geometries and adiabatic excitations for two molecules (NO_2 and SiO). The best estimate of the vertical excitation and the geometry for BeH ($r_e = 1.326903$) is from the FCI calculation of Pitrach-Ruiz et al.[135] The geometries (in Å and deg) for CO ($r_{CO} = 1.128$), H_2CO ($r_{CO} = 1.203$,

$r_{CH} = 1.102$, $\theta_{HCO} = 121.9$), N_2 ($r_{NN} = 1.098$), and H_2O ($r_{OH} = 0.957$, $\theta_{HOH} = 104.5$) are taken from Handy and Tozer.[133] The reference vertical excitation energies for N_2, CO, and H_2CO are from experiments,[136−138] whereas the reference vertical excitation energy for H_2O is determined in the present study by using high-level WFT calculations. The reference adiabatic excitation energy for SiO is taken from NIST Chemistry Webbook,[134] whereas that for NO_2 is taken from a benchmark calculation of Bera et al.[139]

3. Computational Methods

3.1. Geometries and Basis Sets. The basis sets and geometries used for the training sets and test sets in the present article are listed in Table 1. The 6−311+G(2df,2p),[140−142] 6−311+G(3df,2p),[140−142] 6−311+G(3df,3pd),[140−142] DIDZ (short name of 6−31+G(d,p)),[142−144] MG3S,[145] MQZVP,[28,146] and aug-cc-pVQZ[147] basis sets are explained elsewhere. A new basis set, MG3SXP, is used for some of the calculations in this study. The MG3SXP (where XP denotes "extra polarization") basis differs from the MG3S[114] basis set in the same way that G3LargeXP differs from G3Large,[148] in particular, the 2df polarization functions of MG3S on Li−Ne are replaced by a 3df set, and the 3d2f polarization functions on Al−Ar are replaced by 4d2f, where the polarization functions are those recommended by Curtiss et al.[148]

3.2. Counterpoise Corrections. For the noncovalent complexes in S22, we performed calculations with and without the counterpoise (CP) corrections[149,150] for basis set superposition error (BSSE). The results for the NCCE31 database are CP corrected, whereas the results for the UUU7 database are CP uncorrected.

3.3. Spin−Orbit Energy. Except for the AE17 database (for which the reference data are from high-level nonrelativistic WFT calculations) and except when explicitly indicated otherwise in Section 5.2.1, the spin−orbit energy is added for all species for which it is nonzero. A complete list of spin−orbit energies used for calculations in this article can be found elsewhere.[151]

3.4. Software. All DFT calculations in this article were performed with a locally modified version of the *Gaussian03* program.[152,153] The high-level WFT calculations that are used to determine the reference vertical excitation energy of H_2O are performed with the *NWChem* program.[154]

3.5. Excitation Energies. The multiplicity-changing excitation energies are not calculated with time-dependent DFT but by taking the energy difference between ground states of different multiplicity.

4. Theory and Parametrization

The local parts of the M08-HX and M08-SO functionals depend on six variables: up-spin and down-spin densities (ρ_α and ρ_β), their density gradients ($\nabla\rho_\alpha$ and $\nabla\rho_\beta$), and spin kinetic energy densities (τ_α and τ_β).

4.1. M08-Type Exchange Functional. The spin-scaling relation[155] for exchange energy allows us to explain the exchange functionals by considering the exchange functional for a spin-unpolarized system for which $\rho = 2\rho_\alpha = 2\rho_\beta$. In the meta-GGA framework, the exchange energy of a spin-unpolarized system can be written as

$$E_x^{GGA}[\rho] = \int d^3r \rho \varepsilon_x^{LDA}(\rho) F_x(s,\tau) \quad (2)$$

where s is the dimensionless reduced density gradient given by

$$s = |\nabla\rho| / [2(3\pi^2)^{1/3}\rho^{4/3}] \quad (3)$$

where ε_x^{LDA} is the local density approximation[2] for the exchange energy per particle, and $F_x(s,\tau)$ is the meta-GGA exchange enhancement factor.

A key element in the exchange functional is the Taylor series coefficient defined by

$$\mu \equiv \lim_{s\to 0}\left(\frac{1}{2}\frac{d^2F_x}{ds^2}\right) \quad (4)$$

The accurate value of this coefficient is well-known, and we will call it μ^{GE} where GE denotes gradient expansion; the accurate value is $10/81 = 0.1235$.[156]

The M08-type exchange functional form is based on our SOGGA exchange functional,[8] which is a half-and-half-mix of the PBE[7] and RPBE[157] exchange functional forms, that is

$$E_x^{SOGGA} = \int dr \rho \varepsilon_x^{LDA}(0.5F_x^{PBE} + 0.5F_x^{RPBE}) \quad (5)$$

where F_x^{PBE} is the enhancement factor for the PBE[7] exchange, and F_x^{RPBE} is the enhancement factor for the RPBE[157] exchange:

$$F_x^{RPBE} = 1 + \kappa_2(1 - e^{-\mu_2 s^2/\kappa_2}) \quad (6)$$

In the present work eq 5 is first generalized to the following local form:

$$E_x^{M08\text{-}Loc} = \int d^3r \rho \varepsilon_x^{LDA}\{f_1(w)F_x^{PBE} + f_2(w)F_x^{RPBE}\} \quad (7)$$

$f_1(w)$ and $f_2(w)$ are the kinetic-energy-density enhancement factors

$$f_1(w) = \sum_{i=0}^{11} a_i w^i \quad (8)$$

$$f_2(w) = \sum_{i=0}^{11} b_i w^i \quad (9)$$

where the variable w is a function of y, and y is a function of the kinetic energy density τ (which equals $2\tau_\alpha$ or $2\tau_\beta$ for a spin-unpolarized system) and density ρ

$$w = (y-1)/(y+1) \quad (10)$$

$$y = \tau^{UEG}/\tau \quad (11)$$

where τ^{UEG} is the Thomas-Fermi[158,159] kinetic energy density for a uniform electron gas (UEG)

$$\tau^{UEG} = \frac{3}{10}(3\pi^2)^{2/3}\rho^{5/3} \quad (12)$$

and

$$\tau = \frac{1}{2}\sum_{i=1}^{n}|\nabla\varphi_i|^2 \quad (13)$$

where φ_i is a generalized Kohn−Sham orbital (also called a Hartree−Fock Kohn−Sham orbital), and n ($\equiv n_\alpha + n_\beta$) is the number of occupied orbitals. (Note that some authors (including ref 160) define τ without the factor of 1/2.)

For a slowly varying density, τ has the gradient expansion (GE)[160]

$$\tau = \tau^{\mathrm{UEG}} + \frac{1}{72}\frac{|\nabla\rho|^2}{\rho} + O(\nabla^2) \quad (14)$$

Using eqs 10−14, we can derive a GE approximation for y and w

$$y^{\mathrm{GE}} \approx \frac{\tau^{\mathrm{UEG}}}{\tau^{\mathrm{UEG}} + \frac{1}{72}\frac{|\nabla\rho|^2}{\rho}} = \frac{1}{1 + \frac{1}{72}\frac{|\nabla\rho|^2}{\rho\tau^{\mathrm{UEG}}}} = \frac{1}{1 + \frac{5}{27}s^2} \approx 1 - \frac{5}{27}s^2 \quad (15)$$

$$w^{\mathrm{GE}} = \frac{y^{\mathrm{GE}} - 1}{y^{\mathrm{GE}} + 1} \approx -\frac{5}{54}s^2 \quad (16)$$

Using eqs 2, 7, 8, 9, and 16, we obtain the gradient expansion of the local part of the M08-type exchange

$$F_{\mathrm{x}}^{\mathrm{M08-2X\ Loc}} \approx a_0 + b_0 + \left[a_0\mu^{\mathrm{PBE}} + b_0\mu_2 - \frac{5}{54}(a_1 + b_1)\right]s^2 \quad (17)$$

Note that by dropping the second term in the parentheses of eq 5, we recover the exchange functional form used for M05-2X and M06-2X, although those functionals have different numerical coefficients than are used here. In eq 6, we use $\mu_2 = 10/81$ (as mentioned above, this is also the second-order expansion coefficient for the exact exchange) and $\kappa_2 = 0.552$; both are the same as used in the SOGGA[8] functional.

4.2. M08-Type Correlation Functional. In the M05-2X and M06-2X correlation functionals, we treat the opposite-spin and parallel-spin correlation differently by using an ansatz of Stoll et al.[161] for the LSDA correlation energies. However, a recent study by Gori-Giorgi and Perdew[162] shows that the Stoll ansatz is inaccurate for a uniform electron gas. Therefore, we do not use the Stoll ansatz in the M08-type functional. We also avoid using the M06-2X self-correlation correction factor, D_σ, which only solves the one- or two-electron self-correlation problem and cannot solve the self-exchange and many-electron self-interaction problems.[163,164] Furthermore, a singularity in D_σ can lead to convergence problems in the self-consistent-field iterations.[165]

The functional form of the M08-type correlation functional is given by

$$E_{\mathrm{C}}^{\mathrm{M08}} = \int d\mathbf{r}\rho\varepsilon_{\mathrm{C}}^{\mathrm{LSDA}}(r_s,\varsigma)f_3(w)d\mathbf{r} + \int d\mathbf{r}\rho H^{\mathrm{PBE}}(r_s,\varsigma,t)f_4(w)d\mathbf{r} \quad (18)$$

where $\varepsilon_{\mathrm{C}}^{\mathrm{LSDA}}(r_s,\varsigma)$ is the correlation energy per electron of the uniform electron gas limit, for which we use the parametrization of Perdew and Wang;[166] $H^{\mathrm{PBE}}(r_s,\varsigma,t)$ is the PBE[7] gradient correction for the correlation, and $f_3(w)$ and $f_4(w)$ are the kinetic-energy-density enhancement factors for correlation

$$f_3(w) = \sum_{i=0}^{11} c_i w^i \quad (19)$$

$$f_4(w) = \sum_{i=0}^{11} d_i w^i \quad (20)$$

The arguments in $\varepsilon_{\mathrm{C}}^{\mathrm{LSDA}}(r_s,\varsigma)$ and $H^{\mathrm{PBE}}(r_s,\varsigma,t)$ are defined by

$$r_{\mathrm{s}} = (3/4\pi\rho) \quad (21)$$

$$\zeta = (\rho_\alpha - \rho_\beta)/(\rho_\alpha + \rho_\beta) \quad (22)$$

$$t = |\nabla\rho|/[4(3/\pi)^{1/6}\rho^{7/6}] \quad (23)$$

4.3. Hybrid Meta Functional. The hybrid meta exchange-correlation energy can be written as follows

$$E_{\mathrm{xc}}^{\mathrm{hyb}} = Y \times E_{\mathrm{x}}^{\mathrm{HF}} + (1 - Y)E_{\mathrm{x}}^{\mathrm{Loc}} + E_{\mathrm{c}}^{\mathrm{DFT}} \quad (24)$$

where $E_{\mathrm{X}}^{\mathrm{HF}}$ is the nonlocal HF exchange energy, Y is $X/100$, X is the percentage of HF exchange in the hybrid functional, $E_{\mathrm{X}}^{\mathrm{Loc}}$ is the local DFT exchange energy, and $E_{\mathrm{C}}^{\mathrm{DFT}}$ is the local DFT correlation energy. The M08-type exchange enhancement factor can formally be written as

$$F_{\mathrm{x}}^{\mathrm{M08}} = YF_{\mathrm{x}}^{\mathrm{HF}} + (1 - Y)F_{\mathrm{x}}^{\mathrm{M08-Loc}} \quad (25)$$

where $F_{\mathrm{x}}^{\mathrm{HF}}$ is the factor implied by HF exchange.

We optimize X along with the parameters in the two M08-type functionals. The optimization procedure is given in the next subsection.

For a slowly varying density, $F_{\mathrm{x}}^{\mathrm{HF}}$ has the second-order gradient expansion[167]

$$F_{\mathrm{x}}^{\mathrm{HF}} = 1 + \mu_2 s^2 + O(\nabla^2) \quad (26)$$

Combining eqs 7, 25, and 26, we obtain the gradient expansion of the M08-type exchange functionals

$$F_{\mathrm{x}}^{\mathrm{M08}} \approx [(1 - Y)(a_0 + b_0) + Y] + \left[(1 - Y)a_0\mu^{\mathrm{PBE}} + (Y + Yb_0)\mu_2 - \frac{5}{54}(1 - Y)(a_1 + b_1)\right]s^2 \quad (27)$$

4.4. Optimization of the New Hybrid Meta-GGA. All parameter optimizations were carried out in a self-consistent fashion. The parameters a_i, b_i, c_i, and d_i in eqs 8, 9, 19, and 20 were determined by fitting to the data in the training set. To obtain the correct UEG limit, according to eqs 11 and 19, we enforce the following constraints in M08-HX:

$$(1-Y)(a_0+b_0) + Y = 1 \quad (28)$$

$$c_0 = 1 \quad (29)$$

For the M08-SO functional, we respect the gradient expansion to the second order in both exchange and correlation. According to eqs 18 and 27, we therefore enforce the following constraints:

$$(1 - Y)a_0\mu^{\mathrm{PBE}} + (Y + (1 - Y)b_0)\mu_2 - \frac{5}{54}(1 - Y)(a_1 + b_1) = \frac{10}{81} \approx 0.1235 \quad (30)$$

$$c_1 = 0 \quad (31)$$

$$d_0 = 1 \quad (32)$$

The constraints in eqs 29, 31, and 32 ensure that the M08-SO correlation functional is correct to the second order for slow varying density because, as discussed elsewhere,[7,168] the PBE correlation functional is correct through the second order.

We optimized the remaining parameters in M08-HX and M08-SO against accurate data to minimize a training function F defined by

$$F = \mathrm{RMSEPB(MGAE109)} + \mathrm{RMSE(IP13)} + \mathrm{RMSE(EA13)} + \mathrm{RMSE(PA8)} + \mathrm{RMSE(DBH76)} + 10 \times \mathrm{RMSE(NCCE31)} + \mathrm{RMSE(ABDE4)} + \mathrm{RMSE(AE17)} + \mathrm{RMSE}(\pi\mathrm{TC13}) \quad (33)$$

where RMSEPB denotes RMSE per bond, and RMSE denotes root-mean-square error. Note that πTC13 is the union of πIE3, PA-P5/06, and PA-SB5/06; all databases are listed in Table 1. As explained in Sections 2 and 3, Table 1 also presents the references for each database and the basis sets and geometries employed in this work for each database. The optimized parameters for M08-HX and M08-SO are listed in Table 2.

Using the optimized parameters in Table 2 and eq 27, we obtain the second-order gradient expansion of the M08-HX exchange

$$F_{\mathrm{x}}^{\mathrm{M08-HX}} \approx 1 + \mu^{\mathrm{M08-HX}} s^2 = 1 + 0.2696 s^2 \quad (34)$$

5. Results and Discussion

We first discuss the performance of the tested functionals for the training set. In some cases we compare to other popular and high-performance functionals;[2,4,5,7−11,14,15,17−28,92,133,166,169−177] these functionals are explained in Table 3. Conventional functionals can be classified according to a ladder of ingredients, and Table 3 also indicates the rung of Jacob's ladder[87,88] to which each functional belongs. LSDA is rung 1, GGAs are rung 2, meta functionals that contains spin kinetic energy density or Laplacians of the density are rung 3 (meta GGAs), hybrid GGAs and hybrid meta functionals are rung 4, and using unoccupied orbitals puts one on rung 5. Some functionals on rung 4 contain rung-3 ingredients, and some do not. To distinguish these they are called respectively hybrid meta, denoted 4 (HM), and hybrid GGA, denoted 4 (HG).

Table 3 also contains a column called μ. This is defined in eq 4 and is worked out using the same methods as in Sections 4.1 and 4.3.

In all tables after Table 3, the functionals will always be given in order of increasing mean unsigned error (MUE) for that table (as given in the last row or column of the table or in the following table). When meaningful, we also give mean signed error (MSE).

5.1. Performance for the Training Sets. Table 4 present the mean errors of M05-2X, M06-2X, M08-HX, M08-SO, and B3LYP for the training data for molecules. The TC-MUE defined in Table 4 is the MUE for the 160 data for main-group thermochemistry, TK-MUE is the MUE for the 76 data for thermochemical kinetics, and NC-MUE is the MUE for the 31 noncovalent data in the training set. The last row is for AMUE, which is the average of TC-MUE, TK-MUE, and NC-MUE. M06-2X gives smaller NC-MUE than M08-HX, and M08-HX gives the smaller TK-MUE. Overall the AMUE for M08-HX is just slightly better than M06-2X. Since we enforced the gradient expansion coefficients to the second order in M08-SO, M08-SO is just slightly worse than M06-2X and M08-HX. As shown by the AMUE in Table 4, M08-SO, M06-2X, and M08-2X perform much better than B3LYP for the molecular training set.

Table 5 lists the TC-MUEs, TK-MUEs, NC-MUEs, and AMUEs for 29 functionals and for HF theory and a column for the number of optimized parameters in each functional, including parameters inherited from incorporated functional forms, even if they are not re-optimized. Table 5 shows that LSDA performs better than HF theory for the TC and NC areas, but it is inferior to HF for kinetics. The SOGGA functional,[8] which has been designed for lattice constants in solid-state physics and to illustrate the results with a correct

Table 3. Complete List of Functionals Used in This Article[a]

method	rung	X	μ[b]	refs
B1B95	4 (HM)	28	0.2321	9
B2PLYP	5	53	0.1944	83
B3LYP	4 (HG)	20	0.2222	4,5,14,15
B3LYP*	4 (HG)	15	0.2160	174
B3P86	4 (HG)	20	0.2222	5, 14,170
B3PW91	4 (HG)	20	0.2222	5,14,171
B88[c]	2	0	0.2743	5
B97−1	4 (HG)	21	0.1654	172
B97−2	4 (HG)	21	0.0376	175
B97−3	4 (HG)	26.93	0.1044	19
B98	4 (HG)	21.98	0.1244	92
BB1K	4 (HM)	42	0.2109	23
BLYP	2	0	0.2743	4,5
BMK	4 (HM)	42	1.1112	25
BP86	2	0	0.2743	5, 170
HCTH	2	0	−0.1260	172
HFLYP	4 (HG)	100	0.1235	176
LSDA	1	0	0.0000	2,166,169
M05	4 (HM)	28	0.1872	26
M05-2X	4 (HM)	56	0.1889	27
M06	4 (HM)	27	0.1762	28
M06-2X	4 (HM)	54	0.1881	28
M06-HF	4 (HM)	100	0.0900	177
M06-L	3	0	0.2678	11
M08-HX	4 (HM)	52.23	0.2696	this work
M08-SO	4 (HM)	56.79	0.1235	this work
MPW1B95	4 (HM)	31	0.12(0.23) [d]	24
MPW1K	4 (HG)	42	0.12 (0.21) [d]	20
mPW1PW[e]	4 (HG)	25	0.12(0.24) [d]	17
mPW2PLYP	5	55	0.12 (0.19)[d]	90
MPW3LYP	4 (HG)	20	0.12 (0.25) [d]	24
MPWB1K	4 (HM)	44	0.12 (0.21)[d]	24
OLYP	2	0	0.0000	4,133
PBE	2	0	0.2195	7
PBEh[f]	4 (HG)	25	0.1955	18
PW91	2	0	0.12 (0.27) [d]	171
SOGGA	2	0	0.1235	8
TPSS	3	0	0.1235	10
TPSSh	4 (HM)	10	0.1235	22
VSXC[e]	3	0	0.0982	173
τ-HCTHh	4 (HM)	15	0.0733	21

[a] Hartree−Fock theory (which could be considered as a fourth-rung functional but here is considered to be a form of wave function theory (WFT)) is not included in this table. [b] The second-order gradient expansion coefficient for the exchange enhancement factor. [c] B88 denotes using Becke's 1988 exchange functional (the same exchange functional that is used in BLYP) with no correlation functional. [d] See ref 8. [e] Also called mPW1PW91, mPW0, and MPW25. [f] Also called PBE1PBE and PBE0. [g] Also called VS98.

Table 4. Statistical Errors (kcal/mol) for the Molecular Training Data

database	M08-HX MSE	M08-HX MUE	M06-2X MSE	M06-2X MUE	M08-SO MSE	M08-SO MUE	M05-2X MSE	M05-2X MUE	B3LYP MSE	B3LYP MUE
MGAE109	−0.20	0.39	−0.18	0.40	−0.24	0.44	−0.02	0.48	−0.69	0.91
IP13	3.20	3.37	1.06	2.54	3.13	3.53	1.69	3.54	3.58	4.72
EA13	−0.79	1.36	1.30	2.07	−2.72	2.76	0.53	2.03	−1.51	2.29
PA8	0.23	1.01	−0.19	1.75	−0.52	1.57	−0.25	1.23	0.18	1.02
ABDE4	−0.49	0.62	0.27	0.74	0.52	2.30	−0.18	0.61	−8.62	8.62
πIE3	2.77	2.77	1.63	1.63	2.06	2.06	2.99	2.99	6.24	6.24
PA-P5	0.16	0.46	0.37	0.66	1.48	1.48	2.07	2.07	5.79	5.79
PA-SB5	2.50	2.50	1.69	2.00	1.47	1.88	3.90	3.90	5.90	5.90
TC-MUE[a]		0.86		0.86		1.09		1.10		1.94
HTBH38[b]	0.00	0.73	−0.51	1.13	−0.51	1.09	−0.39	1.34	−4.13	4.23
HATBH12[b]	−0.96	1.72	−0.81	1.61	−1.30	1.84	1.15	2.00	−8.49	8.49
NSBH16[b]	0.63	1.10	0.77	1.22	0.23	1.06	−0.79	1.48	−3.25	3.25
UABH10[b]	0.39	1.00	0.32	0.92	0.27	1.15	0.91	1.77	−1.42	2.02
TK-MUE[c]		1.00		1.20		1.21		1.53		4.40
HB6[d]	−0.03	0.31	−0.14	0.25	0.06	0.23	−0.05	0.20	−0.93	0.93
CT7[d]	0.06	0.32	−0.01	0.27	0.19	0.50	0.13	0.30	0.30	0.54
DI6[d]	−0.01	0.28	−0.12	0.31	0.09	0.20	−0.15	0.32	−0.94	0.94
WI7[d]	−0.02	0.09	0.06	0.09	−0.03	0.05	0.00	0.03	−0.39	0.39
PPS5[d]	−0.42	0.45	−0.33	0.39	−0.30	0.43	−0.69	0.71	−3.19	3.19
NC-MUE[e]		0.28		0.25		0.28		0.29		1.09
AMUE		0.71		0.77		0.86		0.97		2.48

[a] This is the MUE for MGTC160. [b] HTBH38, HATBH12, NSBH16, and UABH10 are components of DBH76 as explained in refs 11 and 28. [c] This is the MUE for DBH76. [d] HB6, CT7, DI6, WI7, and PPS5 are components of NCCE31, as explained in refs 28 and 113. [e] This is the MUE for NCCE31.

Table 5. Statistical Errors (kcal/mol) for the Molecular Training Data

functionals	rung	no. of parameters[a]	TC-MUE	TK-MUE	NC-MUE	AMUE
M08-HX	4 (HM)	47	0.86	1.00	0.28	0.71
M06-2X	4 (HM)	35	0.86	1.20	0.25	0.77
M08-SO	4 (HM)	44	1.09	1.21	0.28	0.86
M05-2X	4 (HM)	22	1.10	1.53	0.29	0.97
BMK	4 (HM)	20	1.25	1.29	1.12	1.22
MPWB1K	4 (HM)	7	1.74	1.37	0.65	1.25
M06	4 (HM)	38	1.28	2.13	0.41	1.28
M06-HF	4 (HM)	38	1.33	2.25	0.42	1.33
M05	4 (HM)	22	1.54	2.03	0.44	1.34
BB1K	4 (HM)	6	2.07	1.29	1.18	1.51
MPW1B95	4 (HM)	7	1.37	2.66	0.67	1.57
B97−3	4 (HG)	19	1.69	1.87	1.19	1.58
B1B95	4 (HM)	6	1.40	2.53	1.26	1.73
MPW1K	4 (HG)	5	3.07	1.55	0.87	1.83
B97−2	4 (HG)	16	1.77	2.74	1.22	1.91
B98	4 (HG)	16	1.61	3.78	0.73	2.04
mPW1PW	4 (HG)	5	1.91	3.39	0.89	2.07
B97−1	4 (HG)	16	1.63	3.93	0.66	2.07
PBEh	4 (HG)	1	1.78	3.87	0.67	2.11
M06-L	3	39	1.92	4.02	0.58	2.17
B3LYP	4 (HG)	7	1.94	4.40	1.09	2.48
MPW3LYP	4 (HG)	8	1.83	5.02	0.80	2.55
τ-HCTHh	4 (HM)	20	1.78	4.92	1.47	2.73
TPSSh	4 (HM)	1	2.18	6.44	1.03	3.21
TPSS	3	0	2.17	8.33	1.19	3.90
BLYP	2	4	2.45	8.31	1.58	4.11
PBE	2	0	3.15	8.92	1.10	4.39
HFLYP	4 (HG)	3	7.84	7.08	0.76	5.22
SOGGA	2	0	6.31	11.45	2.12	6.63
LSDA	1	0	13.45	15.13	2.17	10.25
HF	NA[a]	0	26.48	7.71	2.62	12.27

[a] Number of independent optimized parameters in each functional. This does not include hidden parameters (such as the choice of a functional form that makes a term in the gradient expansion vanish for empirical reasons) or parameters that are fitted to accurate calculations of the correlation energy of a uniform electron gas. [b] NA denotes "not applicable".

second-order gradient expansion, performs better than LSDA for all three areas, but it is not as good for main-group

Table 6. Statistical Errors (kcal/mol) for Atomic Training Data (AE17)

method	X[a]	MSE	MUE
Results with the aug-cc-pVQZ Basis Set			
M06-2X	54	0.61	2.00
M08-HX	52.23	−0.70	4.05
M06	27	0.33	4.37
B98	21.98	3.08	5.02
B97−1	21	2.03	5.38
M06-L	0	−5.25	5.61
M08-SO	56.79	4.82	5.71
τ-HCTHh	15	0.69	6.04
M06-HF	100	−5.58	6.20
B97−3	26.93	2.83	6.61
M05-2X	56	−7.88	7.89
HFLYP	100	−7.61	8.37
MPW1K	42	−8.52	9.22
B97−2	21	−8.74	9.69
mPW1PW	25	−8.82	9.77
M05	28	−7.04	9.98
BLYP	0	−9.29	10.05
TPSSh	10	−14.32	14.32
BB1K	42	−13.45	14.74
B1B95	28	−13.73	15.19
MPWB1K	44	−13.44	15.32
MPW1B95	31	−13.69	15.94
B3LYP	20	−16.90	16.90
TPSS	0	−16.94	16.94
MPW3LYP	20	−16.98	16.98
BMK	42	17.77	18.24
PBEh	25	39.48	39.57
PBE	0	48.81	48.81
B88	0	190.46	190.46
HF	100	191.97	191.97
SOGGA	0	284.46	284.46
LSDA	0	425.54	425.54
Results with Other Basis Sets			
M06-2X/MQZVP	54	−0.73	1.76
M06-2X/MG3S	54	4.38	4.52
M05-2X/MG3S	56	−3.86	4.83
M05-2X/MQZVP	56	−9.27	9.29

[a] Percentage of Hartree−Fock exchange in each functional.

Table 7. Statistical Errors (kcal/mol) for the G3-3AE75 Database[a]

methods	rung	MaxE+	MaxE-	MSE	MUE
		with Spin−Orbit			
M08-HX/MG3SXP	4 (HM)	8.2 ($C_4H_4N_2$)	−8.6 (SO_3)	−0.54	2.28
M08-HX/6−311++G(3df,3pd)	4 (HM)	8.7 ($C_4H_4N_2$)	−12.5 (SO_3)	0.11	2.54
M06-2X/6−311++G(3df,3pd)	4 (HM)	17.8 (P_4)	−9.9 (SO_3)	0.70	2.72
M06-SO/MG3SXP	4 (HM)	8.9 ($C_4H_4N_2$)	−12.4 (SF_6)	−1.41	2.76
M06-2X/MG3SXP	4 (HM)	15.5 (P_4)	−6.7 (SO_3)	−0.38	2.86
M05-2X/MG3SXP	4 (HM)	16.6 (P_4)	−8.2 (SO_3)	3.47	4.11
TPSS/6−311++G(3df,3pd)[b]	4 (HM)	12.3 ($C_4H_4N_2$)	−9.4 (PF_5)	4.19	4.76
B3LYP/6−311+G(3df,3pd)[b]	4 (HG)	4.5 ($C_4H_4N_2$)	−23.7 (SF_6)	−9.23	9.39
		without Spin−Orbit			
M08-HX/MG3SXP	4 (HM)	8.5 ($C_4H_4N_2$)	−7.3 (SO_3)	0.46	2.31
M08-HX/6−311++G(3df,3pd)	4 (HM)	9.0 ($C_4H_4N_2$)	−11.2 (SO_3)	1.10	2.79
M08-SO/MG3SXP	4 (HM)	9.2 ($C_4H_4N_2$)	−9.6 (SF_6)	−0.42	2.68
M06-2X/MG3SXP	4 (HM)	15.5 (P_4)	−5.8 ($Si(CH_3)_4$)	0.61	2.95
M06-2X/6−311++G(3df,3pd)	4 (HM)	17.8 (P_4)	−8.7 (SO_3)	1.70	3.06
M05-2X/MG3SXP	4 (HM)	16.6 (P_4)	−6.9(SO_3)	4.46	4.90
		Results from Literature (without Spin−Orbit)			
Mpw2plyp-D[d]	5	5.9 ($C_4H_4N_2$)	−9.1 (P_4)	−0.40	2.11
B2PLYP-D[d]	5	6.8 ($C_4H_4N_2$)	−8.7 ($Si(CH_3)_4$)	−0.74	2.21
TPSSh[c]	4 (HM)	6.6 (C_8H_{18})	−16.2 (PF5)	−0.16	3.33
mPW2PLYP[d]	5	4.8 ($C_4H_4N_2$)	−9.6 ($Si(CH_3)_4$)	−2.96	3.39
B2PLYP[d]	5	5.2 ($C_4H_4N_2$)	−13.6 ($Si(CH_3)_4$)	−4.27	4.67
VSXC[c]	3	8.7 (C_6H_5)	−12.0 (C_8H_{18})	−1.97	4.74
B3PW91[c]	4 (HG)	17.0 (naphthalene)	−17.0 (PF_5)	2.54	4.87
LC-ωPBE[e]	4	N. A.[f]	N. A.[f]	2.05	5.28
TPSS[c]	3	12.8 (S_2Cl_2)	−7.5 (PF_5)	5.19	5.48
OLYP[c]	2	11.0 (CF_3)	−20.9 ($Si(CH_3)_4$)	−6.41	7.91
B3LYP[c]	4 (HG)	4.9 ($C_4H_4N_2$)	−20.8 (SF_6)	−8.23	8.44
HCTH[c]	2	22.2 (C_2F_6)	−27.5 ($Si(CH_3)_4$)	−6.38	10.18
PBE0[c]	4 (HG)	35.6 (naphthalene)	−14.5 (PF_5)	9.28	10.20
BPW91[c]	2	28.0 (azulene)	−22.4 ($Si(CH_3)_4$)	4.97	11.08
PKZB[c]	3	11.0 (P_4)	−35.4 (PF_5)	−10.59	11.24
BLYP[c]	2	11.0 ($C_4H_4N_2$)	−41.0 (C_8H_{18})	−12.42	13.88
PBE[c]	2	79.7 (azulene)	none	32.77	32.77
PW91[c]	2	81.1 (azulene)	none	35.25	35.25
BP86[c]	2	72.7 (azulene)	none	38.61	38.61
B3P86[c]	3	79.2 (C_8H_{18})	none	41.89	41.89
LSDA[c]	1	347.5 (azulene)	none	197.11	197.1
HF[c]	NA		−582.2 (C_8H_{18})	−336.4	336.4

[a] B3LYP/6−31G(2df,p) geometries are used. [b] Calculated from the raw energies in the Supporting Information of ref 22. [c] Taken from ref 22. [d] Calculated from the results in the Supporting Information of ref 90. [e] Calculated from the results in ref 70. [f] N. A. denotes "not available". The maximum errors for LC-ωPBE were not reported in ref 70.

energetics as PBE and BLYP, which are the most popular functionals on rung 2. The M06-L meta GGA, a third-rung functional, outperforms the most popular hybrid GGA, which is the fourth-rung B3LYP functional. Table 5 shows that B97−3 is the best performing hybrid GGA for the molecular training set, and BMK is the best performing non-Minnesota functional.

With 13 more semiempirical parameters, the AMUE of M06-2X is 0.2 kcal/mol smaller than that of M05-2X, whereas it is just 0.06 kcal/mol greater than the AMUE of M08-HX with 12 less semiempirical parameters. Furthermore, M06-2X has 9 less parameters than the M08-SO functional, but M06-2X outperforms M08-SO by a small margin. Tables 4 and 5 indicate that an AMUE of ∼0.7 kcal/mol is the limit of accuracy of the hybrid meta functionals for this set of 267 molecular data.

Table 6 lists the mean errors for the atomic training data. As shown in this table, M06-2X performs better than M08-HX and M08-SO for atomic energies. The results do not correlate with the percentage of Hartree−Fock exchange.

5.2. Performance for the Test Sets. In this section, we present tests against some databases which are outside of our training set.

5.2.1. G3-3AE75 Database. Table 7 presents the mean signed errors (MSEs) and mean unsigned errors (MUEs) for the molecules in the G3-3 database. The G3-3 data set[33] contains molecules as large as naphthalene and multihalogen-containing molecules such as SF_6 and PF_5. The tests for this database in the literature employed the 6−311++G(3df,3pd) basis set without spin−orbit energies. To make a consistent comparison, we calculated the MUEs and MSEs with and without spin−orbit energies for the M06-2X, M08-HX, TPSS, and B3LYP functionals.

Table 7 shows that including spin−orbit energies improves the performance of M06-2X and M08-HX by 0.1−0.3 kcal/mol but deteriorates the performance of M08-SO by ∼0.1 kcal/mol. (Nevertheless spin−orbit coupling is a real effect, and it should always be included. Except for Table 6 and the bottom section of Table 7, all other results in this paper and in our previous work (except when comparing to theoretical nonrelativistic data for atoms) include spin−orbit

Table 8. Results for the LMAE14 Database (kcal/mol)

molecule	exp.	M08-HX	M08-SO	M06-2X	M05-2X	B3LYP
C_6F_6	1389.9	1398.2	1397.4	1406.4	1410.1	1383.7
C_6F_5Cl	1365.1	1373.0	1371.8	1379.7	1383.1	1353.5
dodecane $C_{12}H_{26}$	3655.4	3651.1	3647.6	3648.0	3659.3	3622.9
hexadecane $C_{16}H_{34}$	4833.7	4827.3	4822.7	4823.1	4837.9	4786.1
adamantane $C_{10}H_{16}$	2695.1	2693.7	2691.8	2690.3	2702.9	2657.7
diadamantane $C_{14}H_{20}$	3624.9	3624.6	3622.3	3620.1	3639.1	3568.2
pyrene $C_{16}H_{10}$	3301.9	3298.6	3294.8	3302.8	3319.6	3273.7
fluroanthene $C_{16}H_{10}$	3286.7	3284.3	3281.0	3288.1	3304.5	3259.5
anthracene $C_{14}H_{10}$	2952.8	2949.9	2946.8	2953.5	2967.8	2930.9
phenazine $C_{12}H_8N_2$	2693.2	2700.2	2698.0	2698.6	2711.3	2683.5
azobenzene $C_{12}H_{10}N_2$	2793.6	2797.5	2796.2	2795.4	2807.7	2782.1
benzophenone $C_{13}H_{10}O$	2882.3	2881.8	2879.5	2884.8	2896.4	2861.5
dibenzothiophene $C_{12}H_8S$	2562.7	2561.1	2558.2	2562.7	2576.0	2536.5
dithiin $C_{16}H_{12}S_2$	3503.1	3510.4	3508.1	3511.5	3529.1	3472.9
MSE		0.8	−1.7	1.7	14.6	−26.3
MUE		4.1	5.5	5.7	14.6	26.3

[a] M06-L/6−311+G(2df,2p) geometries are used.

energy for cases where it is nonzero.) M08-HX performs better than M06-2X especially when using the MG3SXP basis. M06-2X, M08-SO, and M08-2X outperform the B2-PLYP and mPW2-PLYP functionals, but they underperform the B2-PLYP-D and mPW2PLYP-D functionals. The ability of the fourth-rung M06-2X, M08-SO, and M08-2X functionals to compete with fifth-rung functionals is very encouraging.

5.2.2. LMAE14 Database. Table 8 present the results for the LMAE14 database. This is a data set of large molecules, and B3LYP gives an error of 26.2 kcal/mol for this database, whereas M08-HX gives an MUE of only 4.1 kcal/mol. M06-2X, with an MUE of 5.7 kcal/mol, is less accurate than M08-SO and M08-HX. O3LYP is the best functional for this database in the test of Curtiss et al.,[118] with an MUE of 8.6 kcal/mol, but this is larger than that for M08-HX by more than a factor of 2; this illustrates the tremendous progress that has been made in the last four years. The results for this database show that M08-HX does improve upon M06-2X for large molecules.

5.2.3. IE34 Database. Tables S2 and 9 present the results for the isomerization energy database. The changes in structure and bonding for the 34 isomerizations are notably diverse and potentially challenging. B3LYP gives a large error for octane isomerization (Table S1, entry 11), and Grimme[39,44] also pointed out the inability of most popular functionals to describe this type of stereoelectronic effect. M06-2X, M08-SO, and M08-HX perform well for describing the stereoelectronic effects in hydrocarbons, as does M05-2X.[94] M06-2X performs poorly for reactions involving three-member-ring molecules (Table S1, entries 3, 8, 16, and 25), and two M08 functionals perform better in these cases.

The statistical errors for IE34 are given in Table 9. We also include the results for the best performing GGA, hybrid GGA, meta-GGA, and doubly hybrid functional and a WFT method in the test of Grimme et al.[45] Table 9 shows that M06-HX gives a smaller MUE and RMSE than M06-2X. The number of outliers for the two M08 functionals is also less than that for M06-2X.

Table 9 also shows that M06-2X and two M08 functionals are more accurate than mPW2-PLYP for the IE34 database, but they are less accurate than SCS-MP2, the best performing method in Table 10, which is a WFT method for which the computation for an N-atom system scales as N^5 whereas the conventional algorithm for hybrid functional scales as N^4, and density fitting algorithm for rungs 1−3 have a scaling of N^3.

Table 9. Statistical Errors for the IE34 Database

method	rung	MaxE	no. outliers[a]	RMSE	MUE
M08-HX	4 (HM)	3.1 (33)	2	1.44	1.12
M08-SO	4 (HM)	3.2 (16)	1	1.52	1.15
M06-2X	4 (HM)	4.3 (8)	4	1.65	1.15
M05-2X	4 (HM)	4.6 (27)	2	1.74	1.31
B3LYP	4 (HG)	10.1 (12)	9	3.22	2.28
Results from Literature					
SCS-MP2[b,c]	WFT	2.6 (2)	0	1.27	1.03
mPW2PLYP[b]	5	6.1 (12)	4	1.83	1.19
BMK[b]	4 (HM)	4.7 (7)	4	1.79	1.28
PBE0[b]	4 (HG)	7.0 (11)	7	2.45	1.79
PBE[b]	2	7.3 (11)	6	2.54	1.89
TPSS[b]	3	11.4 (27)	10	3.46	2.52

[a] Number of unsigned errors >3.0 kcal/mol. [b] Taken from ref 45. [c] WFT: wave function theory (not DFT).

5.2.4. Noncovalent Databases. The ability of the new generation of hybrid meta density functionals[13,24,27,28,113] to treat noncovalent interaction energies that are dominated by medium-range correlation is a major step forward in the usefulness of DFT for practical simulation on biological systems and soft materials. Table 10 shows, for example, that two M08 functionals and M06-2X reduce the error for the "dispersion dominated" complexes of the S22 database by an order of magnitude, as compared to the popular B3LYP functional. The reduction in error is also significant for the hydrogen bonded ones. In Tables S2 and S3 (Supporting Information), we present results for a double-ζ basis set. We also defined a quantity called mean averaged MUE (MAMUE) in Tables S2 and S3 which is an average over all three types of interactions and over CP-corrected and uncorrected results. Table S3 presents the MAMUEs for 34 functionals. If we use MAMUE to rank these functionals, we can see that the best performing GGA is SOGGA, the best performing meta-GGA is M06-L, and the best performing hybrid meta GGAs are M06-2X, M08-SO, and M08-HX.

Table 10. Results (kcal/mol) for the S22 Database

complex	best estimate	MP2/CBS	M06-2X CP	M06-2X noCP	M08-SO CP	M08-SO noCP	M08-HX CP	M08-HX noCP	B3LYP CP	B3LYP noCP
Hydrogen Bonded (HB) Complexes										
$(NH_3)_2$	−3.2	−3.2	−3.2	−3.3	−3.2	−3.3	−3.4	−3.6	−2.2	−2.3
$(H_2O)_2$	−5.0	−5.0	−5.1	−5.4	−5.1	−5.4	−5.1	−5.6	−4.5	−4.8
formic acid dimmer	−18.6	−18.6	−18.9	−19.6	−18.4	−18.9	−18.4	−19.3	−17.2	−17.8
formamide dimmer	−16.0	−15.9	−15.6	−16.0	−15.6	−16.0	−15.8	−16.4	−13.9	−14.3
uracil dimer	−20.7	−20.6	−19.4	−19.8	−19.4	−19.8	−19.7	−20.2	−17.8	−18.1
2-pyridoxine·2-aminopyridine	−16.7	−17.4	−15.5	−15.8	−15.1	−15.5	−15.5	−16.0	−13.7	−14.0
adenine·thymine WC	−16.4	−16.5	−15.0	−15.3	−14.5	−15.0	−15.0	−15.5	−12.8	−13.1
MSE-HB		−0.1	0.5	0.2	0.7	0.4	0.5	0.0	1.9	1.3
MUE-HB		0.1	0.7	0.6	0.8	0.6	0.6	0.6	2.0	1.6
Dispersion Dominated (DD) Complexes										
$(CH_4)_2$	−0.5	−0.5	−0.4	−0.5	−0.5	−0.5	−0.3	−0.3	0.4	0.4
$(C_2H_4)_2$	−1.5	−1.6	−1.6	−1.7	−1.8	−2.0	−1.9	−2.0	0.5	0.5
benzene·CH_4	−1.5	−1.9	−1.5	−1.7	−1.6	−2.1	−1.8	−2.3	0.8	0.6
benzene dimer	−2.7	−5.0	−2.8	−3.7	−3.0	−4.2	−3.0	−4.5	3.8	3.0
pyrazine dimer	−4.4	−6.9	−4.2	−4.8	−4.2	−5.0	−4.2	−5.2	2.6	2.0
uracil dimer	−10.1	−11.4	−9.9	−11.1	−9.3	−10.7	−9.3	−11.2	−0.9	−1.9
indole·benzene	−5.2	−8.1	−4.6	−5.7	−4.8	−6.2	−4.8	−6.6	4.8	3.9
adenine·thymine stack	−12.2	−14.9	−12.2	−13.4	−11.8	−13.2	−11.8	−13.7	1.5	0.5
MSE		−1.5	0.1	−0.6	0.2	−0.7	0.2	−1.0	6.5	5.9
MUE		1.5	0.2	0.6	0.3	0.7	0.4	1.0	6.5	5.9
Mixed Complexes										
ethene·ethyne	−1.5	−1.7	−1.4	−1.5	−1.5	−1.7	−1.6	−1.9	−0.6	−0.8
benzene·H_2O	−3.3	−3.6	−3.6	−4.1	−3.7	−4.2	−3.7	−4.4	−1.2	−1.7
benzene·NH_3	−2.4	−2.7	−2.4	−2.7	−2.5	−2.9	−2.7	−3.1	−0.1	−0.4
benzene· HCN	−4.5	−5.2	−4.9	−5.4	−5.3	−5.9	−5.4	−6.2	−2.0	−2.4
benzene dimer	−2.7	−3.6	−2.4	−2.9	−2.5	−3.2	−2.4	−3.3	1.0	0.5
indole·benzene T-shape	−5.7	−7.0	−5.1	−5.8	−5.2	−6.1	−5.2	−6.3	−0.5	−1.1
phenol dimer	−7.1	−7.8	−6.6	−7.1	−6.6	−7.1	−6.6	−7.3	−2.9	−3.4
MSE-mixed	−0.6	0.1	−0.3	0.0	−0.6	−0.1	−0.8	3.0	2.6	
MUE-mixed		0.6	0.4	0.3	0.4	0.6	0.4	0.8	3.0	2.6
AMUE[b]		0.8	0.4	0.5	0.5	0.6	0.5	0.8	3.8	3.3

[a] The 6−311+G(3df,2p) basis set is used for all calculations. [b] Average of the MUEs for three types of noncovalent complexes.

Table 11. Interaction Energies (kcal/mol) in the UUU7 Database[a]

	best estimate[b]	M08-SO	M06-2X	M08-HX	M05-2X	B3LYP
HB/HB 1	−37.8	−37.78	−37.80	−38.68	−38.11	−34.70
HB/HB 2	−37.4	−36.86	−36.49	−37.44	−36.81	−32.31
T/T 1	−36.6	−36.02	−36.20	−36.60	−35.82	−25.80
HB/HB 3	−33.5	−33.38	−33.10	−33.97	−33.46	−30.08
S/T 1	−33.2	−32.96	−33.34	−34.01	−30.98	−17.68
HB/S 1	−32.8	−32.83	−33.38	−33.98	−31.01	−17.87
S/S 1	−20.1	−19.94	−20.51	−21.00	−17.06	1.15
MSE		0.23	0.08	−0.61	1.08	10.59
MUE		0.24	0.40	0.61	1.37	10.59

[a] See Figure 1 for the structures for the peptides. [b] Calculated from the results in ref 122.

Table 11 presents results for interaction energies in large uracil trimers. Table 11 shows that the improvements for the uracil trimer database are even greater than those for S22. In particular, M08-HX, M06-2X, and M08-SO have MUEs respectively 17, 26, and 44 times lower than B3LYP.

5.2.5. APCE5 Database. Table 12 compares four density functionals and one DFT-D method for the aromatic peptide conformational energy database. The mean unsigned error for M05-2X, M08-HX, and M08-SO is only 22% higher than that for the functional with explicit dispersion corrections (TPSS-D), and it is four times smaller than B3LYP's mean unsigned error.

5.2.6. BBH7/08 Database. One goal of our development efforts is to design a density functional with accurate performance for a broad range of observables, and the prediction of barrier heights is a central concern. These reactions are chosen to include singlets, doublets, and triplets and some highly correlated systems, like C_2H, so they provide a significant challenge. The performance for the new benchmark barrier heights in Table 13 is very encouraging, especially in that the M06-2X and M08-2X functionals are more accurate than B3LYP for all the reactions that involve the multireference C_2H molecule. These three functionals have $X = 54$, 54, and 20, respectively. Although any functional with X as large as 20 (or larger) is not expected to be reliable for multireference systems, it is encouraging that the M06-2X and M08-HX give useful accuracy in these difficult cases. Further study of cases with multireference character is a worthwhile goal.[178]

The mean unsigned error of M06-2X, 1.06 kcal/mol, is better than the value, 1.20 kcal/mol, obtained for DBH76 (Table 4), and the mean unsigned error for M08-HX, 0.86 kcal/mol, is outstanding again improving on the value (1.0 kcal/mol in Table 4) for DBH76.

5.2.7. Internuclear Distances. The hybrid meta functionals M05-2X, M06-2X, M08-SO, and M08-2X have a high Hartree−Fock exchange (the percentage, X, of Hartree−Fock exchange is greater than 50%), and, as a consequence, they do not improve on B3LYP for bond lengths in small molecules, as shown in Table S4 (in the Supporting Information). Among the three high-X functionals, M08-HX and

Table 12. Conformational Energies (kcal/mol) in the APCE5 Database[a]

	best estimate[b]	TPSS-D[b]	M05-2X	M08-HX	M08-SO	M06-2X	TPSS[b]	B3LYP
WG_12-WG_01	2.45	2.41	2.28	1.90	1.54	1.70	4.96	5.22
WGG_13-WGG_01	4.24	5.35	3.79	2.58	2.81	2.48	9.00	9.32
FGG_300-FGG_099	3.12	1.49	1.01	3.27	2.99	2.72	−3.35	−3.82
GGF_01-GGF_15	2.93	2.89	1.82	1.62	1.48	1.50	4.00	3.88
GFA_16-GFA_15	1.56	1.22	1.66	1.83	1.79	1.55	0.79	1.56
MSE		−0.19	−0.75	−0.62	−0.74	−0.87	0.22	0.37
MUE		0.63	0.79	0.79	0.83	0.87	3.12	3.15

[a] See Figure 2 for the structures for the peptides. [b] Calculated from the results in the Supporting Information of ref 121.

Table 13. Barrier Heights (kcal/mol) in the BBH7 Database

reaction	best estimate	M08-HX	M06-2X	M08-SO	M05-2X	B3LYP
$CH_3 + CH_4 \rightarrow CH_4 + CH_3$	17.82	17.47	16.80	17.47	16.88	15.65
$HCC + HCCH \rightarrow HCCH + CCH$	12.79	12.27	13.15	11.20	10.27	9.13
$OH^- + CH_3OH \rightarrow CH_3OH + OH^-$	14.40	14.23	14.17	15.54	12.66	11.37
$HCC + H_2 \rightarrow HCCH + H$	2.07	1.27	1.93	0.25	0.03	0.12
$HCCH + H \rightarrow HCC + H_2$	32.32	34.49	31.67	35.25	35.04	30.33
$O + CH_4 \rightarrow OH + CH_3$	14.19	13.04	11.80	13.53	10.95	7.21
$OH + CH_3 \rightarrow O + CH_4$	9.12	8.26	6.36	8.63	5.47	4.48
MSE		−0.24	−0.98	−0.12	−1.63	−3.49
MUE		0.86	1.08	1.28	2.41	3.49

M08-SO perform better than M05-2X and M06-2X for bond lengths in small molecules.

Both medium-range correlation energies and repulsive interactions play important roles in large crowded molecules, such as cyclophanes,[123,179] and so they provide challenging tests of density functionals. For example, B3LYP gives large errors[124] for internuclear distances in cyclophanes.[180] Table S5 compares the calculated internuclear distances in 2,6,15-trithia-*in*-[3,[4,10]][7]metacyclophane to the experimental results of Pascal et al.[123] The results for PBE, B3LYP, and MP2 were taken from Grimme.[124] Table S5 shows that B3LYP overestimates the internuclear distances in this cyclophane, whereas the popular WFT method MP2 underestimates them. Both M08-HX and M06-2X outperform B3LYP and MP2 by a large margin for the prediction of internuclear distances in this cyclophane. Table S6 compares the calculated internuclear distances in [2,2]paracyclophane to the experimental results.

Table S6 shows the same trends as in Table S5. Note that the M06-L and PBEh functionals performs fairly well for both cylcophanes.

It is instructive to average the errors over some of the key distances in the cyclophanes, in particular we consider C1−C2, C3−C14, and C4−C13 of Figure 4 and C4−C8, C4−C9, and H(C4)-C9 of Figure 3. The mean signed errors in Å are −0.03 Å for MP2, +0.05 Å for B3LYP, +0.03 Å for PBE and TPSS, +0.007 Å for M06-L, +0.006 Å for M06-2X, −0.005 Å for M08-HX, and −0.004 Å for M08-SO. The excellent performance of the new functionals is especially striking since Grimme[124] had concluded that "an explicit account of dispersive-type electron correlation effects between the clamped aromatic units is essentially for a quantitative description of cylcophane structures". The new functionals contain dispersion-like and steric exchange repulsion effects implicitly rather than as explicit molecular mechanics additions.

Table 14 averages the errors in bond lengths over small molecules and two cyclophanes in the second to last column, and it presents the average of the MUEs for MGBL24 and CID15 in the last column. Table 14 shows that the best performers are M06-L and PBEh, followed by M08-HX, M08-SO, SOGGA, M05-2X, and M06-2X.

Table 14. Statistical Errors (Å) for Bond Lengths

method	rung	X	μ	MGBL24[a]	CID15[b]	MGBL34[c]	AMUE[d]
M06-L	3	0	0.2678	0.007	0.008	0.006	0.007
PBEh	4 (HG)	25	0.1955	0.009	0.007	0.008	0.008
M08-HX	4 (HM)	52.23	0.2696	0.013	0.007	0.011	0.010
M08-SO	4 (HM)	56.79	0.1235	0.014	0.006	0.011	0.010
SOGGA	2	0	0.1235	0.014	0.007	0.011	0.010
M05-2X	4 (HM)	56	0.1889	0.016	0.006	0.013	0.011
M06-2X	4 (HM)	54	0.1881	0.015	0.006	0.012	0.011
TPSSh	4 (HM)	10	0.1235	0.012	0.012	0.011	0.012
TPSS	3	0	0.1235	0.015	0.018	0.015	0.017
B97−1	4 (HG)	21	0.1654	0.010	0.023	0.010	0.017
PBE	2	0	0.2195	0.014	0.020	0.013	0.017
BMK	4 (HM)	42	1.1112	0.016	0.020	0.015	0.018
B3LYP	4 (HG)	20	0.2222	0.011	0.026	0.011	0.018

[a] MUE of the MGBL24 database of Table S4. [b] MUE of the 15 bond lengths in Tables S5 and S6. [c] Average of MGBL24 and CID15. [d] MUE of the 34 bond distances in MGBL24 and CID15, that is all 24 distances in MGBL24 and the 10 smallest distances of CID15 (the other five distances in CID15 are nonbonded distances).

Table 15. Scale Factor and Statistical Errors (cm^{-1}) for the F38 Database

	B3LYP	M08-SO	M08-HX	M06-2X	M05-2X
MSE	8	20	44	49	64
MUE	31	52	56	56	70
scale factor	0.998	0.995	0.984	0.982	0.975
MSE after scaling	4	9	9	9	8
MUE after scaling	31	51	49	45	44

5.2.8. Frequencies. M06-2X and the two M08 functionals do not improve on B3LYP for frequencies in small molecules, as shown in Tables S7 and 15. We also optimized a scale factor for harmonic frequencies for each of the tested functionals, with the optimization being to improve the harmonic frequencies, as in ref 28. After scaling, the MUE

Table 16. Vertical Excitation Energies (VEE) for H_2O (kcal/mol)[a]

method	$^1A_1 \rightarrow {}^3B_1$
CCSD(T)/aug-cc-pVTZ	167.58
CCSD(T)/aug-cc-pVQZ	168.68
CCSDT/aug-cc-pVTZ	167.37
$CCSDT(2)_Q$/aug-cc-pVTZ	167.44
Q(TZ)[b]	−0.13
CCSD(T)/aug-cc-pVQZ+Q(TZ)	168.55

[a] At the experimental[133] geometry: $r_{OH} = 0.957$, $\theta_{HOH} = 104.5$ [b] Q(TZ) = VEE($CCSDT(2)_Q$/aug-cc-pVTZ) − VEE(CCSD(T)/aug-cc-pVTZ).

of M06-2X and M08-HX decrease by 11 and 7 cm^{-1}, respectively.

5.2.9. Multiplicity-Changing Excitation Energies. For transitions to electronic states with a different multiplicity from the ground state, we calculated the excitation energy by performing self-consistent-field (SCF) calculations on both states. The reference vertical excitation energy for H_2O is calculated by using the CCSD(T)/aug-cc-pVQZ+Q(TZ) method, where Q(TZ) stands for the quadruple excitation correlation contributions calculated at the $CCSDT(2)_Q$ level[181] of theory. Table 16 summarizes the WFT results for the vertical excitation of H_2O, with some results from the literature.

Besides the best estimates and the M06-2X, M08-HX, M08-SO, B3LYP, and M05-2X results, we also present the multiplicity-changing excitation energies for nine other methods in Table 17. Two of the methods, BMK and B97-3, are chosen for comparison because in previous tests[28] on 41 diverse excitations (23 of which conserve multiplicity and 18 of which do not) these two methods showed the best mean performance of any of the non-Minnesota functionals that were tested. The other methods in Table 17 illustrate the effect of introducing empirical parameters for exchange and correlation in the set of functionals built on B88 exchange, HF exchange, and LYP correlation.

Table 17 shows that the new M08-HX functional is the best performer for the multiplicity-changing excitation energy excitation energy database, followed by B97-3, BMK, M08-SO, and M06-2X. The B3LYP*, B3LYP, BLYP, HFLYP, B88, and HF functionals in Table 17 show the effects of several different ways to mix and scale the components of a hybrid GGA. HF has 100% HF exchange with no correlation energy; B88 has 100% B88 exchange with no correlation energy. HFLYP has 100% HF exchange with 100% LYP correlation energy; BLYP has 100% B88 exchange with 100% LYP correlation energy. B3LYP has 20% HF exchange, 72% B88 exchange, and 80% LSDA exchange with 81% LYP correlation energy, and B3LYP* has 15% HF exchange, 72% B88 exchange, and 85% LSDA exchange with 81% LYP correlation energy. The results obtained for these six functionals show several features that merit further consideration. First of all, HF exchange is often said to relatively overstablize high-spin states, and Table 17 shows that, in comparison to experiment, HFLYP underestimates the excitation energy to a high-multiplicity state in eight out of nine cases. Furthermore, as compared to B88, HF underestimates the excitation energy to a high-spin state in seven of nine cases. These results confirm expectations. Next, however, compare B88 to HFLYP. Although exchange has usually been considered to be the key to correct multiplicity ordering and spin-state splitting,[174,182−191] the difference in MUE between HFLYP and HF is larger than the difference between B88 and HF, showing the importance of differential dynamical correlation for spin-state splitting. Another "surprise" is found by comparing B3LYP to B3LYP*, a functional that was developed by Reiher and co-workers[174,182] especially to improve multiplicity-changing excitation energies by decreasing the weighting of HF exchange since the HF theory underestimates spin-state splittings. Table 17 shows that, as compared to B3LYP, sometimes B3LYP* predicts higher spin-state splitting and sometimes lower; on average it is only slightly more accurate than B3LYP.

5.2.10. Discussion of μ. In general the orbitals, like the Hartree−Fock exchange functional, are nonlocal functions of the density, so a local functional of the orbitals brings in some nonlocal information and is sometimes called semilocal.[192] However in our classification (which is also used by some other workers—there is no consensus on the language), any functional that depends only on local values of the spin densities, their gradient magnitudes, and the spin kinetic energy densities is called local. Functionals that are not local are called nonlocal or hybrid. To the best of our knowledge, μ values have not been presented previously for hybrid functionals, so the comparison of μ values in Table 3 merits some discussion.

It has been known for a long time that the value of μ can be helpful in understanding the performance of GGAs, and it has sometimes been stated that functionals with the gradient-expansion value (that is $\mu_{GE} = 10/81 \approx 0.1246$) of μ should be more accurate for solids and surfaces, whereas those with values about twice as high should be more accurate for free atoms and small molecules.[192−196] Our recent study[8] provided a more nuanced conclusion, namely that using $\mu \approx \mu_{GE}$ leads to better accuracy for interatomic spacings not only in solids but also in molecules, at least for bond lengths that do not involve hydrogens, whereas $\mu \approx 2\ \mu_{GE}$ leads to better accuracy not only for atomization energies of molecules but also for barrier heights of chemical reactions and cohesive energies of solids.

It is impossible for a single GGA to be highly accurate for both interatomic spacings and energetics. Adding orbital dependencies such as Hartree−Fock exchange and kinetic energy densities can ameliorate this situation. Comparing eq 3 to 14 shows that τ and s bring in similar information in the slow-varying density limit, but the use of τ at finite values of s allow one to distinguish different kinds of electron density regions that have the same s and ρ. Because the explicit dependence on spin kinetic energy densities allows one to distinguish different regions with the same s and ρ, the performance of the hybrid meta functionals does not correlate with μ in the same way as for GGAs. One might ultimately prefer a functional with $\mu = \mu^{GE}$ (as in M08-SO, TPSS, TPSSh, and SOGGA), but so far only M08-SO performs as well for chemistry as do M05-2X, M06-2X, and

Table 17. Multiplicity-Changing Excitation Energies (kcal/mol)[a]

transition	Mg $^1S \rightarrow {}^3P$	Be $^1S \rightarrow {}^3P$	H_2CO $^1A_1 \rightarrow {}^3A_2$	BeH $^2\Sigma_1 \rightarrow {}^4\Pi_2$	CO $^1\Sigma^+ \rightarrow {}^3\Pi$	H_2O $^1A_1 \rightarrow {}^3B_1$	N_2 $^1\Sigma_g^+ \rightarrow {}^3\Sigma_u^+$	NO_2[b] $^2A_1 \rightarrow {}^4A_2$	SiO[b] $^1\Sigma^+ \rightarrow {}^3\Sigma^+$	MSE	MUE
best estimate	62.47	62.84	80.71	134.67	145.74	168.55	178.72	83.30	96.15		
M08-HX	64.66	60.63	80.32	139.85	145.99	170.29	186.91	81.50	95.78	1.42	2.48
B97−3	64.09	56.13	77.83	136.94	142.05	168.92	180.76	79.26	93.25	−1.55	2.95
BMK	61.11	52.97	79.19	134.13	145.84	170.08	185.41	77.99	96.94	−1.06	3.08
M08-SO	65.32	61.90	80.81	143.00	146.60	168.13	187.26	79.36	98.05	1.92	3.10
M06−2X	69.86	63.12	80.82	143.14	142.39	170.18	185.77	79.18	95.73	1.89	3.65
B3LYP*	64.35	56.55	76.13	139.46	140.91	164.04	176.67	79.88	92.46	−2.52	4.00
B3LYP	64.11	56.61	75.86	140.01	140.87	163.43	177.35	77.81	92.41	−2.74	4.29
BLYP	65.46	56.81	76.53	140.28	140.82	163.58	173.91	81.66	91.24	−2.54	4.45
M06-L	60.76	53.39	77.09	81.98	91.64	139.18	136.33	170.56	174.50	−3.08	4.53
M05-2X	75.03	65.98	79.69	141.16	147.30	174.34	186.74	79.18	98.72	3.89	5.03
M06-HF	70.59	70.12	85.65	147.79	147.41	170.50	191.95	77.08	98.31	5.14	6.52
HFLYP	60.23	56.57	65.56	141.12	138.23	155.94	158.77	36.35	93.59	−11.86	13.30
B88	46.47	37.62	70.80	113.97	127.42	146.60	167.68	70.52	79.16	−16.99	16.99
HF	41.20	37.28	58.08	114.87	121.83	137.67	148.42	35.46	80.02	−26.48	26.48

[a] The reference vertical excitation energy for H_2O is the result from CCSD(T)/aug-cc-pVQZ + Q(TZ) in Table 21. See Section 2.2.12 for the source of reference data for other molecules or atoms. [b] These are adiabatic excitation energies; others are vertical excitation energies.

M08-HX; these three functionals have μ values that are 1.52−2.18 times larger than μ_{GE}.

Table 3 shows that M08-HX has a larger value of μ than M05-2X or M06-2X (0.2696 vs 0.1885−0.1889), whereas previous work[8] shows that for GGAs, functionals with even smaller μ (0.1235) predict more accurate nonhydrogenic bond distances. Nevertheless our strategy of allowing a more flexible functional form to allow the resulting functional to be simultaneously more accurate for both energetics and bond distances did succeed in that M08-HX, although fit only to energetics and although more accurate on average than either M05-2X or M06-2X for energetics, is also significantly more accurate for typical bond distances (see Table 14). In fact, functionals with high HF exchange are usually expected to be less accurate than low-X functionals for bond distances, but M08-HX outperforms not only TPSS and PBE, which have $X = 0$, but also SOGGA, which not only has $X = 0$ but also has $\mu = \mu^{GE}$ which is known from previous work to be associated with good accuracy for lattice constants and nonhydrogenic bond distances.

6. Concluding Remarks

This paper presents two new hybrid meta-GGA exchange-correlation functionals, M08-2X and M08-SO, for main-group thermochemistry, thermochemical kinetics, and noncovalent interactions. The new M08-HX functional has an improved functional form as compared to our previous M06-2X and M05-2X functional forms. The M08 functional form rigorously enforces the UEG limit and avoids the use of a self-correlation correction term, which sometimes causes difficulties in the SCF iterations. The M08-HX, M08-SO, M06-2X, and M05-2X functionals have been comparatively assessed against 164 energetic test data, 39 bond lengths, and 38 frequencies outside of the training set.

Before summarizing what we learn from the present research, we remind the readers that since M08-2X, M06-2X, and M05-2X have high Hartree−Fock exchange, they are not parametrized to be suitable for studying many problems in transition metal chemistry or other problems with high multireference character.

From the assessment, we draw the following conclusions:

1) The limit of accuracy of a global hybrid meta-GGA for our training set of 267 molecular data is about 0.75 kcal/mol.

2) M08-HX, M08-SO, and M06-2X perform very well for a combination of main-group thermochemistry, kinetics, and noncovalent interactions.

3) M08-HX, M08-SO, and M06-2X give good performances for the noncovalent interactions in large uracil trimers and for conformational energies in small aromatic peptides.

4) M08-HX, M08-SO, M06-2X, and M05-2X do not improve upon B3LYP for bond lengths in small molecules, but they perform well in predicting the bond lengths in cyclophanes, for which B3LYP fails.

5) M08-2X, M08-SO, M06-2X, and M05-2X do not improve upon B3LYP for frequencies.

6) M08-SO is considerably more accurate for main-group thermochemistry than any previously available functional with the correct second-order behavior in the regime of slowly varying density.

7) The new M08-HX functional has the best performance of tested functionals for several of the databases, in particular, main-group atomization energies, large-molecule atomization energies, electron affinities, hydrogen-transfer barrier heights, heavy-atom transfer barrier heights, new benchmark barrier heights, noncovalent interaction energies in uracil trimers, and multiplicity-changing excitation energies.

Acknowledgment. This work was supported in part by the Air Force Office of Scientific Research (orbital-dependent density functionals), by the National Science Foundation under grant no. CHE07-04974 (complex systems), by the Office of Naval Research under award number N00014-05-0538 (software tools), and by a Molecular Science Computing Facility Computational Grand Challenge grant at the Environmental Molecular Science Laboratory of Pacific Northwestern National Laboratory.

Supporting Information Available: Isomerization energies (Table S1), results for a double-ζ basis set (Tables

S2 and S3), bond lengths (Table S4), internuclear distances (Tables S5 and S6), frequencies (Table S7), and Cartesian coordinates (Tables S8-S11). This material is available free of charge via the Internet at http://pubs.acs.org.

References

(1) Scuseria, G. E.; Staroverov, V. N. In *Theory and Application of Computational Chemistry: The First 40 Years*; Dykstra, C. E., Frenking, G., Kim, K. S., Scuseria, G. E., Eds.; Elsevier: Amsterdam, 2005; p 669.

(2) Kohn, W.; Sham, L. J. *Phys. Rev.* **1965**, *140*, 1133.

(3) Langreth, D. C.; Mehl, M. J. *Phys. Rev. B* **1983**, *28*, 1809.

(4) Lee, C.; Yang, W.; Parr, R. G. *Phys. Rev. B* **1988**, *37*, 785.

(5) Becke, A. D. *Phys. Rev. A* **1988**, *38*, 3098.

(6) Perdew, J. P.; Chevary, J. A.; Vosko, S. H.; Jackson, K. A.; Pederson, M. R.; Singh, D. J. *Phys. Rev. B* **1992**, *46*, 6671.

(7) Perdew, J. P.; Burke, K.; Ernzerhof, M. *Phys. Rev. Lett.* **1996**, *77*, 3865.

(8) Zhao, Y.; Truhlar, D. G. *J. Chem. Phys.* **2008**, *128*, 184109.

(9) Becke, A. D. *J. Chem. Phys.* **1996**, *104*, 1040.

(10) Tao, J.; Perdew, J. P.; Staroverov, V. N.; Scuseria, G. E. *Phys. Rev. Lett.* **2003**, *91*, 146401.

(11) Zhao, Y.; Truhlar, D. G. *J. Chem. Phys.* **2006**, *125*, 194101.

(12) Gruning, M.; Gritsenko, O.; Baerends, E. J. *J. Phys. Chem. A* **2004**, *108*, 4459.

(13) Zhao, Y.; Truhlar, D. G. *Acc. Chem. Res.* **2008**, *41*, 157.

(14) Becke, A. D. *J. Chem. Phys.* **1993**, *98*, 5648.

(15) Stephens, P. J.; Devlin, F. J.; Chabalowski, C. F.; Frisch, M. J. *J. Phys. Chem.* **1994**, *98*, 11623.

(16) Sousa, S. F.; Fernandes, P. A.; Ramos, M. J. *J. Phys. Chem. A* **2007**, *111*, 10439.

(17) Adamo, C.; Barone, V. *J. Chem. Phys.* **1998**, *108*, 664.

(18) Adamo, C.; Barone, V. *J. Chem. Phys.* **1999**, *110*, 6158.

(19) Keal, T. W.; Tozer, D. J. *J. Chem. Phys.* **2005**, *123*, 121103.

(20) Lynch, B. J.; Fast, P. L.; Harris, M.; Truhlar, D. G. *J. Phys. Chem. A* **2000**, *104*, 4811.

(21) Boese, A. D.; Handy, N. C. *J. Chem. Phys.* **2002**, *116*, 9559.

(22) Staroverov, V. N.; Scuseria, G. E.; Tao, J.; Perdew, J. P. *J. Chem. Phys.* **2003**, *119*, 12129.

(23) Zhao, Y.; Lynch, B. J.; Truhlar, D. G. *J. Phys. Chem. A* **2004**, *108*, 2715.

(24) Zhao, Y.; Truhlar, D. G. *J. Phys. Chem. A* **2004**, *108*, 6908.

(25) Boese, A. D.; Martin, J. M. L. *J. Chem. Phys.* **2004**, *121*, 3405.

(26) Zhao, Y.; Schultz, N. E.; Truhlar, D. G. *J. Chem. Phys.* **2005**, *123*, 161103.

(27) Zhao, Y.; Schultz, N. E.; Truhlar, D. G. *J. Chem. Theory Comput.* **2006**, *2*, 364.

(28) Zhao, Y.; Truhlar, D. G. *Theor. Chem. Acc.* **2008**, *120*, 215.

(29) Becke, A. D. *Int. J. Quantum Chem.* **1983**, *23*, 1915.

(30) Becke, A. D. *J. Chem. Phys.* **1998**, *109*, 2092.

(31) Becke, A. D. *J. Chem. Phys.* **2000**, *112*, 4020.

(32) Schmider, H. L.; Becke, A. D. *THEOCHEM* **2000**, *527*, 51.

(33) Curtiss, L. A.; Raghavachari, K.; Redfern, P. C.; Pople, J. A. *J. Chem. Phys.* **2000**, *112*, 7374.

(34) Woodcock, H. L.; Schaefer, H. F.; Schreiner, P. R. *J. Phys. Chem. A* **2002**, *106*, 11923.

(35) Check, C. E.; Gilbert, T. M. *J. Org. Chem.* **2005**, *70*, 9828.

(36) Cerny, J.; Hobza, P. *Phys. Chem. Chem. Phys.* **2005**, *7*, 1624.

(37) Izgorodina, E. I.; Coote, M. L.; Radom, L. *J. Phys. Chem. A* **2005**, *109*, 7558.

(38) Carlier, P. R.; Deora, N.; Crawford, T. D. *J. Org. Chem.* **2006**, *71*, 1592.

(39) Grimme, S. *Angew. Chem., Int. Ed.* **2006**, *45*, 4460.

(40) Schreiner, P. R.; Fokin, A. A., Jr.; de Meijere, A. *Org. Lett.* **2006**, *8*, 3635.

(41) Wodrich, M. D.; Corminboeuf, C.; Schleyer, P. v. R. *Org. Lett.* **2006**, *8*, 3631.

(42) Izgorodina, E. I.; Coote, M. L. *J. Phys. Chem A.* **2006**, *110*, 2486.

(43) Izgorodina, E. I.; Coote, M. L. *Chem. Phys.* **2006**, *324*, 96.

(44) Grimme, S.; Steinmetz, M.; Korth, M. *J. Chem. Theory Comput.* **2007**, *3*, 42.

(45) Grimme, S.; Steinmetz, M.; Korth, M. *J. Org. Chem.* **2007**, *72*, 2118.

(46) Schreiner, P. R. *Angew. Chem., Int. Ed.* **2007**, *46*, 4217.

(47) Izgorodina, E. I.; Brittain, D. R. B.; Hodgson, J. L.; Krenske, E. H.; Lin, C. Y.; Namazian, M.; Coote, M. L. *J. Phys. Chem. A* **2007**, *111*, 10754.

(48) Paier, J.; Marsman, M.; Kresse, G. *J. Chem. Phys.* **2007**, *127*, 24103.

(49) Csonka, G. I.; Ruzsinszky, A.; Perdew, J. P.; Grimme, S. *J. Chem. Theory Comput.* **2008**, *4*, 888.

(50) Paesani, F.; Gianturco, F. A.; Lewerenz, M. *J. Chem. Phys.* **1999**, *111*, 6897.

(51) Ortmann, F.; Schmidt, W. G.; Bechstedt, F. *Phys. Rev. Lett.* **2005**, *95*, 186101.

(52) Grimme, S. *J. Comput. Chem.* **2006**, *27*, 1787.

(53) Jurecka, P.; Cerny, J.; Hobza, P.; Salahub, D. R. *J. Comput. Chem.* **2007**, *28*, 555.

(54) Becke, A. D.; Johnson, E. R. *J. Chem. Phys.* **2006**, *124*, 174104.

(55) Puzder, A.; Dion, M.; Langreth, D. C. *J. Chem. Phys.* **2006**, *124*, 164105.

(56) Sato, T.; Tsuneda, T.; Hirao, K. *J. Chem. Phys.* **2007**, *126*, 234114.

(57) Morgado, C. A.; McNamara, J. P.; Hillier, I. H.; Burton, N. A.; Vincent, M. A. *J. Chem. Theory Comput.* **2007**, *3*, 1656.

(58) Tapavicza, E.; Lin, I.-C.; Lilienfeld, O. A. v.; Tavernelli, I.; Coutinho-Neto, M. D.; Rothlisberger, U. *J. Chem. Theory Comput.* **2007**, *3*, 1673.

(59) Cerny, J.; Jurecka, P.; Hobza, P.; Valdes, H. *J. Phys. Chem. A* **2007**, *111*, 1146.

(60) Antony, J.; Grimme, S. *Phys. Chem. Chem. Phys.* **2006**, *8*, 5287.

(61) Grimme, S.; Antony, J.; Schwabe, T.; Mueck-Lichtenfeld, C. *Org. Biomol. Chem.* **2007**, *5*, 741.

(62) Morgado, C.; Vincent, M. A.; Hillier, I. H.; Shan, X. *Phys. Chem. Chem. Phys.* **2007**, *9*, 448.

(63) Grimme, S. *J. Comput. Chem.* **2004**, *25*, 1463.

(64) Grimme, S.; Mueck-Lichtenfeld, C.; Antony, J. *J. Phys. Chem. C* **2007**, *111*, 11199.

(65) Becke, A. D.; Johnson, E. R. *J. Chem. Phys.* **2007**, *127*, 124108.

(66) Savin, A. In *Recent Developments and Applications of Modern Density Functional Theory*; Seminario, J., Ed.; Elsevier: Amsterdam, 1996; p 327.

(67) Heyd, J.; Scuseria, G. E. *J. Chem. Phys.* **2003**, *118*, 8207.

(68) Yanai, T.; Tew, D. P.; Handy, N. C. *Chem. Phys. Lett.* **2004**, *393*, 51.

(69) Gerber, I. C.; Ángyán, J. G. *Chem. Phys. Lett.* **2005**, *415*, 100.

(70) Vydrov, O. A.; Scuseria, G. E. *J. Chem. Phys.* **2006**, *125*, 234109. /1.

(71) Song, J.-W.; Tokura, S.; Sato, T.; Watson, M. A.; Hirao, K. *J. Chem. Phys.* **2007**, *127*, 154109.

(72) Goll, E.; Werner, H.-J.; Stoll, H. *Chem. Phys.* **2008**, *346*, 257.

(73) Chai, J.-D.; Martin, H.-G. *J. Chem. Phys.* **2008**, *128*, 84106.

(74) Jaramillo, J.; Scuseria, G. E.; Ernzerhof, M. *J. Chem. Phys.* **2003**, *118*, 1068.

(75) Arbuznikov, A. V.; Kaupp, M.; Bahmann, H. *J. Chem. Phys.* **2006**, *124*, 204102.

(76) Bahmann, H.; Rodenberg, A.; Arbuznikov, A. V.; Kaupp, M. *J. Chem. Phys.* **2007**, *126*, 11103.

(77) Janesko, B. G.; Scuseria, G. E. *J. Chem. Phys.* **2007**, *127*, 164117.

(78) Kaupp, M.; Bahmann, H.; Arbuznikov, A. V. *J. Chem. Phys.* **2007**, *127*, 194102.

(79) Arbuznikov, A. V.; Kaupp, M. *Chem. Phys. Lett.* **2007**, *440*, 160.

(80) Janesko, B. G.; Scuseria, G. E. *J. Chem. Phys.* **2008**, *128*, 84111.

(81) Zhao, Y.; Lynch, B. J.; Truhlar, D. G. *J. Phys. Chem A* **2004**, *108*, 4786.

(82) Zhao, Y.; Lynch, B. J.; Truhlar, D. G. *Phys. Chem. Chem. Phys.* **2005**, *7*, 43.

(83) Grimme, S. *J. Chem. Phys.* **2006**, *124*, 34108.

(84) Schwabe, T.; Grimme, S. *Phys. Chem. Chem. Phys.* **2006**, *8*, 4398.

(85) Tarnopolsky, A.; Karton, A.; Sertchook, R.; Vuzman, D. *J. Phys. Chem A* **2008**, *112*, 3.

(86) Benighaus, T.; DiStasio, R. A.; Lochan, R. C.; Chai, J.-D.; Head-Gordon, M. *J. Phys. Chem A* **2008**, *112*, 2702.

(87) Perdew, J. P.; Schmidt, K. In *Density Functional Theory and Its Applications to Materials*; Van-Doren, V., Alsenoy, C. V., Geerlings, P., Eds.; American Institute of Physics: New York, 2001; p 1.

(88) Perdew, J. P.; Ruzsinszky, A.; Tao, J.; Staroverov, V. N.; Scuseria, G. E.; Csonka, G. I. *J. Chem. Phys.* **2005**, *123*, 62201.

(89) Angyan, J. G.; Gerber, I. C.; Savin, A.; Toulouse, J. *Phys. Rev. A* **2005**, *72*, 012510.

(90) Schwabe, T.; Grimme, S. *Phys. Chem. Chem. Phys.* **2007**, *9*, 3397.

(91) Becke, A. D. *J. Chem. Phys.* **1997**, *107*, 8554.

(92) Schmider, H. L.; Becke, A. D. *J. Chem. Phys.* **1998**, *108*, 9624.

(93) Zhao, Y.; Truhlar, D. G. *J. Phys. Chem. A* **2006**, *110*, 10478.

(94) Zhao, Y.; Truhlar, D. G. *Org. Lett.* **2006**, *8*, 5753.

(95) Zhao, Y.; Truhlar, D. G. *J. Org. Chem.* **2007**, *72*, 295.

(96) Zhao, Y.; Truhlar, D. G. *J. Chem. Theory Comput.* **2007**, *3*, 289.

(97) Amin, E. A.; Truhlar, D. G. *J. Chem. Theory Comput.* **2008**, *4*, 75.

(98) Zhao, Y.; Truhlar, D. G. *J. Phys. Chem. A* **2008**, *112*, 1095.

(99) Zhao, Y.; Truhlar, D. G. *J. Phys. Chem. C* **2008**, *112*, 6860.

(100) Dahlke, E. E.; Olson, R. M.; Leverentz, H. R.; Truhlar, D. G. *J. Phys. Chem. A* **2008**, *112*, 3976.

(101) Wodrich, M. D.; Corminboeuf, C.; Schreiner, P. R.; Fokin, A. A.; Schleyer, P. v. R. *Org. Lett.* **2007**, *9*, 1851.

(102) Rokob, T. A.; Hamza, A.; Papai, I. *Org. Lett.* **2007**, *9*, 4279.

(103) Shields, A. E.; van Mourik, T. *J. Phys. Chem A* **2007**, *111*, 13272.

(104) Pietra, F. *J. Phys. Org. Chem.* **2007**, *20*, 1102.

(105) Santoro, F.; Barone, V.; Improta, R. *J. Comput. Chem.* **2008**, *29*, 957.

(106) Brancato, G.; Rega, N.; Barone, V. *Phys. Rev. Lett.* **2008**, *100*, 107401.

(107) Improta, R.; Berisio, R.; Vitagliano, L. *Protein Sci.* **2008**, *17*, 955.

(108) Ellingson, B. A.; Truhlar, D. G. *J. Am. Chem. Soc.* **2007**, *129*, 12765.

(109) Hayama, T.; Baldridge, K. K.; Wu, Y.-T.; Linden, A.; Siegel, J. S. *J. Am. Chem. Soc.* **2008**, *130*, 1583.

(110) Zhao, Y.; Truhlar, D. G. *J. Phys. Chem. C* **2008**, *112*, 4061.

(111) Zhao, Y.; Truhlar, D. G. *J. Am. Chem. Soc.* **2007**, *129*, 8440.

(112) Zhao, Y.; Truhlar, D. G. *Phys. Chem. Chem. Phys.* **2008**, *10*, 2813.

(113) Zhao, Y.; Truhlar, D. G. *J. Phys. Chem. A* **2005**, *109*, 5656.

(114) Lynch, B. J.; Zhao, Y.; Truhlar, D. G. *J. Phys. Chem. A* **2003**, *107*, 1384.

(115) Zhao, Y.; González-García, N.; Truhlar, D. G. *J. Phys. Chem. A* **2005**, *109*, 2012 (E) **2006**, *110*, 4942.

(116) Zhao, Y.; Truhlar, D. G. *J. Chem. Theory Comput.* **2005**, *1*, 415.

(117) Chakravorty, S. J.; Gwaltney, S. R.; Davidson, E. R.; Parpia, F. A.; Fischer, C. F. F. *Phys. Rev. A* **1993**, *47*, 3649.

(118) Curtiss, L. A.; Redfern, P. C.; Raghavachari, K. *J. Chem. Phys.* **2005**, *123*, 124107.

(119) Sattelmeyer, K. W.; Tirado-Rives, J.; Jorgensen, W. L. *J. Phys. Chem A* **2006**, *110*, 13551.

(120) Jurecka, P.; Sponer, J.; Cerny, J.; Hobza, P. *Phys. Chem. Chem. Phys.* **2006**, *8*, 1985.

(121) Valdes, H.; Pluhackova, K.; Pitonak, M.; Rezac, J.; Hobza, P. *Phys. Chem. Chem. Phys.* **2007**, *10*, 2497.

(122) Kabelác, M.; Sherer, E. C.; Cramer, C. J.; Hobza, P. *Chem. Eur. J.* **2006**.

(123) Pascal, R. A.; Winans, C. G.; Engen, D. V. *J. Am. Chem. Soc.* **1989**, *111*, 3007.

(124) Grimme, S. *Chem. Eur. J.* **2004**, *10*, 3423.

(125) Tirado-Rives, J.; Jorgensen, W. L. *J. Chem. Theory Comput.* **2008**, *4*, 297.

(126) Hobza, P.; Sponer, J. *Chem. Rev.* **1999**, *99*, 3247.

(127) Hobza, P.; Sponer, J. *J. Am. Chem. Soc.* **2002**, *124*, 11802.

(128) Martin, J. M. L.; Oliveira, G. D. *J. Chem. Phys.* **1999**, *111*, 1843.

(129) Zheng, J. J.; Zhao, Y.; Truhlar, D. G. *J. Phys. Chem A* **2007**, *111*, 4632.

(130) Gonzales, J. M.; Allen, W. D.; Schaefer, H. F., III *J. Phys. Chem. A* **2005**, *109*, 10613.

(131) Troya, D. *J. Phys. Chem A* **2007**, *111*, 10745.

(132) *NIST Computational Chemistry Comparison and Benchmark Database*; Johnson, R. D., III, Ed.; 2006. http://srdata.nist.gov/cccbdb/ (accessed July 2008).

(133) Handy, N. C.; Tozer, D. J. *Mol. Phys.* **1998**, *94*, 707.

(134) http://webbook.nist.gov/chemistry/ (accessed July 2008).

(135) Pitarch-Ruiz, J.; Sánchez-Marín, J.; Velasco, A. M. *J. Comput. Chem.* **2008**, *29*, 523.

(136) Ben-Shlomo, S. B.; Kaldor, U. *J. Chem. Phys.* **1990**, *92*, 3680.

(137) Nielsen, E. S.; Jorgensen, P.; Oddershede, J. *J. Chem. Phys.* **1980**, *73*, 6238.

(138) Clouthier, D. J.; Ramsay, D. A. *Annu. Rev. Phys. Chem.* **1983**, *34*, 31.

(139) Bera, P. P.; Yamaguchi, Y.; Henry, F.; Schaefer, I. *J. Chem. Phys.* **2007**, *127*, 174303.

(140) Krishnan, R.; Binkley, J. S.; Seeger, R.; Pople, J. A. *J. Chem. Phys.* **1980**, *72*, 650.

(141) McLean, A. D.; Chandler, G. S. *J. Chem. Phys.* **1980**, *72*, 5639.

(142) Hehre, W. J.; Radom, L.; Schleyer, P. v. R.; Pople, J. A. *Ab Initio Molecular Orbital Theory*; Wiley: New York, 1986.

(143) Hehre, W. J.; Ditchfield, R.; Pople, J. A. *J. Chem. Phys.* **1972**, *56*, 2257.

(144) Francl, M. M.; Petro, W. J.; Hehre, W. J.; Binkley, J. S.; Gordon, M. S.; DeFrees, D. J.; Pople, J. A. *J. Chem. Phys.* **1982**, *77*, 3654.

(145) Lynch, B. J.; Truhlar, D. G. *J. Phys. Chem. A* **2003**, *107*, 3898.

(146) Weigend, F.; Furche, F.; Ahlrichs, R. *J. Chem. Phys.* **2003**, *119*, 12753.

(147) Woon, D. E.; T.H. Dunning, J. *J. Chem. Phys.* **1993**, *98*, 1358.

(148) Curtiss, L. A.; Redfern, P. C.; Raghavachari, K. *J. Chem. Phys.* **2007**, *126*, 84108.

(149) Boys, S. F.; Bernardi, F. *Mol. Phys.* **1970**, *19*, 553.

(150) Schwenke, D. W.; Truhlar, D. G. *J. Chem. Phys.* **1985**, *82*, 2418. 1987, 86, 3760 (E).

(151) Lynch, B. J.; Zhao, Y.; Truhlar, D. G. *J. Phys. Chem. A* **2005**, *109*, 1643.

(152) Frisch, M. J.; Trucks, G. W.; Schlegel, H. B.; Scuseria, G. E.; Robb, M. A.; Cheeseman, J. R.; Montgomery, J. A., Jr.; Kudin, K. N.; Burant, J. C.; Millam, J. M.; Iyengar, S. S.; Tomasi, J.; Barone, V.; Mennucci, B.; Cossi, M.; Scalmani, G.; Rega, N.; Petersson, G. A.; Nakatsuji, H.; Hada, M.; Ehara, M.; Toyota, K.; Fukuda, R.; Hasegawa, J.; Ishida, M.; Nakajima, T.; Honda, Y.; Kitao, O.; Nakai, H.; Klene, M.; Li, X.; Knox, J. E.; Hratchian, H. P.; Cross, J. B.; Adamo, C.; Jaramillo, J.; Gomperts, R.; Stratmann, R. E.; Yazyev, O.; Austin, A. J.; Cammi, R.; Pomelli, C.; Ochterski, J. W.; Ayala, P. Y.; Morokuma, K.; Voth, G. A.; Salvador, P.; Dannenberg, J. J.; Zakrzewski, G.; Dapprich, S.; Daniels, A. D.; Strain, M. C.; Farkas, O.; Malick, D. K.; Rabuck, A. D.; Raghavachari, K.; Foresman, J. B.; Ortiz, J. V.; Cui, Q.; Baboul, A. G.; Clifford, S.; Cioslowski, J.; Stefanov, B. B.; Liu, G.; Liashenko, A.; Piskorz, P.; Komaromi, I.; Martin, R. L.; Fox, D. J.; Keith, T.; Al-Laham, M. A.; Peng, C. Y.; Nanayakkara, A.; Challacombe, M.; Gill, P. M. W.; Johnson, B.; Chen, W.; Wong, M. W.; Gonzalez, C.; Pople, J. A. *Gaussian03; Revision E.01 ed.*; Gaussian, Inc.: Pittsburgh, PA, 2008.

(153) Zhao, Y.; Truhlar, D. G. *MN-GFM: Minnesota Gaussian Functional Module - Version 4.0beta*; University of Minnesota: Minneapolis, MN, 2006.

(154) Bylaska, E. J.; Jong, W. A. d.; Govind, N.; Kowalski, K.; Straatsma, T. P.; Valiev, M.; Wang, D.; Aprà, E.; Windus, T. L.; Hammond, J.; Nichols, P.; Hirata, S.; Hackler, M. T.; Zhao, Y.; Fan, P.-D.; Harrison, R. J.; Dupuis, M.; Smith, D. M. A.; Nieplocha, J.; Tipparaju, V.; Krishnan, M.; Auer, A. A.; Nooijen, M.; Brown, E.; Cisneros, G.; Fann, G. I.; Früchtl, H.; Garza, J.; Hirao, K.; Kendall, R.; Nichols, J. A.; Tsemekhman, K.; Wolinski, K.; Anchell, J.; Bernholdt, D.; Borowski, P.; Clark, T.; Clerc, D.; Dachsel, H.; Deegan, M.; Dyall, K.; Elwood, D.; Glendening, E.; Gutowski, M.; Hess, A.; Jaffe, J.; Johnson, B.; Ju, J.; Kobayashi, R.; Kutteh, R.; Lin, Z.; Littlefield, R.; Long, X.; Meng, B.; Nakajima, T.; Niu, S.; Pollack, L.; Rosing, M.; Sandrone, G.; Stave, M.; Taylor, H.; Thomas, G.; Lenthe, J. v.; Wong, A.; Zhang, Z. *NWChem A Computational Chemistry Package for Parallel Computers; Version 5.1 ed.*; Pacific Northwest National Laboratory: Richland, WA, U.S.A., 2007.

(155) Oliver, G. L.; Perdew, J. P. *Phys. Rev. A* **1979**, *20*, 397.

(156) Antoniewicz, P. R.; Kleinman, L. *Phys. Rev. B* **1985**, *31*, 6779.

(157) Hammer, B.; Hansen, L. B.; Norskov, J. K. *Phys. Rev. B* **1999**, *59*, 7413.

(158) Thomas, L. H. *Proc. Camb. Philos. Soc.* **1927**, *23*, 542.

(159) Fermi, E. *Z. Phys.* **1928**, *48*, 73.

(160) Brack, M.; Jennings, B. K.; Chu, Y. H. *Phys. Lett. B* **1976**, *65*, 1.

(161) Stoll, H.; Pavkidou, C. M. E.; Preuss, H. *Theor. Chim. Acta* **1978**, *49*, 143.

(162) Gori-Giorgi, P.; Perdew, J. P. *Phys. Rev. B* **2004**, *69*, 041103.

(163) Mori-Sánchez, P.; Cohen, A. J.; Yang, W. *J. Chem. Phys.* **2006**, *125*, 201102.

(164) Ruzsinszky, A.; Perdew, J. P.; Csonka, G. I.; Vydrov, O. A.; Scuseria, G. E. *J. Chem. Phys.* **2007**, *126*, 104102.

(165) Gräfenstein, J.; Izotov, D.; Cremer, D. *J. Chem. Phys.* **2007**, *127*, 214103.

(166) Perdew, J. P.; Wang, Y. *Phys. Rev. B* **1992**, *45*, 13244.

(167) Svendesen, P. S.; von Barth, U. *Phys. Rev. B* **1996**, *54*, 17402.

(168) Staroverov, V. N.; Scuseria, G. E.; Tao, J.; Perdew, J. P. *Phys. Rev. B* **2004**, *69*, 75102.

(169) Slater, J. C. *Quantum Theory of Molecular and Solids. Vol. 4: The Self-Consistent Field for Molecular and Solids*; McGraw-Hill: New York, 1974.

(170) Perdew, J. P. *Phys. Rev. B* **1986**, *33*, 8822.

(171) Perdew, J. P. In *Electronic Structure of Solids '91*; Ziesche, P., Eschig, H., Eds.; Akademie Verlag: Berlin, 1991; p 11.

(172) Hamprecht, F. A.; Cohen, A. J.; Tozer, D. J.; Handy, N. C. *J. Chem. Phys.* **1998**, *109*, 6264.

(173) Van Voorhis, T.; Scuseria, G. E. *J. Chem. Phys.* **1998**, *109*, 400.

(174) Reiher, M.; Salomon, O.; Hess, B. A. *Theor. Chem. Acc.* **2001**, *107*, 48.

(175) Wilson, P. J.; Bradley, T. J.; Tozer, D. J. *J. Chem. Phys.* **2001**, *115*, 9233.

(176) Valentin, C. D.; Pacchioni, G.; Bredow, T.; Dominguez-Ariza, D.; Illas, F. *J. Chem. Phys.* **2002**, *117*, 2299.

(177) Zhao, Y.; Truhlar, D. G. *J. Phys. Chem. A* **2006**, *110*, 13126.

(178) Johnson, E. R.; Becke, A. D. *J. Chem. Phys.* **2008**, *128*, 124105.

(179) Pasacal, R. A. *J. Phys. Chem. A* **2001**, *105*, 9040.

(180) Pascal, R. A. *Eur. J. Org. Chem.* **2004**, *18*, 3763.

(181) Hirata, S.; Fan, P.-D.; Auer, A. A.; Nooijen, M.; Piecuch, P. *J. Chem. Phys.* **2004**, *121*, 12197.

(182) Reiher, M. *Inorg. Chem.* **2002**, *41*, 6928.

(183) Poli, R.; Harvey, J. N. *Chem. Soc. Rev.* **2003**, *32*, 1.

(184) Paulsen, H.; Trautwein, A. X. *J. Phys. Chem. Solids* **2004**, *65*, 793.

(185) Fouqueau, A.; Mer, S.; Casida, M. E.; Daku, L.; Max, L.; Hauser, A.; Mineva, T.; Neese, F. *J. Chem. Phys.* **2004**, *120*, 9473.

(186) Paulsen, H.; Trautwein, A. X. *Top. Curr. Chem.* **2004**, *235*, 197.

(187) Swart, M.; Groenhof, A. R.; Ehlers, A. W.; Lammertsma, K. *J. Phys. Chem. A* **2004**, *108*, 5479.

(188) Harvey, J. N. *Struct. Bonding (Berlin)* **2004**, *112*, 151.

(189) Liao, M.-S.; Watts, J. D.; Huang, M.-J. *J. Comput. Chem.* **2006**, *27*, 1577.

(190) Rong, C.; Lian, S.; Yin, D.; Shen, B.; Zhong, A.; Bartolotti, L.; Liu, S. *J. Chem. Phys.* **2006**, *125*, 174102.

(191) Sorkin, A.; Iron, M. A.; Truhlar, D. G. *J. Chem. Theory Comput.* **2008**, *4*, 307.

(192) Kurth, S.; Perdew, J. P.; Blaha, P. *Int. J. Quantum Chem.* **1999**, *75*, 889.

(193) Perdew, J. P.; Constantin, L. A.; Sagvolden, E.; Burke, K. *Phys. Rev. Lett.* **2006**, *97*, 223002.

(194) Csonka, G. I.; Vydrov, O. A.; Scuseria, G. E.; Ruzsinszky, A.; Perdew, J. P. *J. Chem. Phys.* **2007**, *126*, 244107.

(195) Madsen, G. K. H. *Phys. Rev. B* **2007**, *75*, 195108.

(196) Perdew, J. P.; Ruzsinszky, A.; Csonka, G. I.; Vydrov, O. A.; Scuseria, G. E.; Constantin, L. A.; Zhou, X.; Burke, K. *Phys. Rev. Lett.* **2008**, *100*, 136406.

CT800246V